Three thousand years of anthropogenic impact and water management and its impact on the hydro-ecosystem of the Mérantaise river, Paris conurbation (France)

Lucile de Milleville, Laurent Lespez, Agnès Gauthier, Frédéric Gob, Clément Virmoux, Ségolène Saulnier-Copard, Valentine Fichet, Manon Letourneur, Marion Jugie, Marta Garcia, et al.

Three thousand years of anthropogenic impact and water management and its impact on the hydro-ecosystem of the Mérantaise River, Paris conurbation (France).

Lucile de Milleville*[1,2], Laurent Lespez[1,2], Agnès Gauthier[1], Frédéric Gob[1,3], Clément Virmoux[1], Ségolène Saulnier-Copard[1], Valentine Fichet[1], Manon Letourneur[1,2,3], Marion Jugie[4], Marta Garcia[5], Kazuyo Tachikawa[5], Evelyne Tales[6]

[1]Laboratoire de Géographie Physique (LGP), CNRS, UMR 8591, 2 rue Henri Dunant, 94320 Thiais, France.

[2]Université de Paris-Est Créteil (UPEC), 61 avenue du Général de Gaulle, 94010 Créteil Cedex France.

[3]Université de Paris1 Panthéon-Sorbonne, Institut de Géographie, 191 rue Saint-Jacques 75005 Paris, France.

[4] Vallons de Haute Bretagne Communauté, 35580 GUICHEN

[5]Centre Européen de Recherche et d'Enseignement des Géosciences de l'Environnement (CEREGE), technopole environnement arbois-méditerranée BP80 13545 Aix-en-Provence, cedex 04, France.

[6]Institut National de Recherche pour l'Agriculture, l'Alimentation et l'Environnement (INRAE), Equipe HYCAR, 1 Rue Pierre Gilles de Gennes, 92160 Antony.

*Corresponding author lucile.demilleville@lgp.cnrs.fr

Highlights

- Degradation of aquatic environments over the last 1,500 years around Paris.
- Anthropic impact on the fluvial system from the Iron Age.
- Palaeobiological and sedimentological signature of hemp retting Early Middle Age
- Environmental impact of mill ponds and agropastoral practices during Middle Ages
- Evidence of organic pollution and eutrophication from the Early Medieval Age.

Graphical abstract

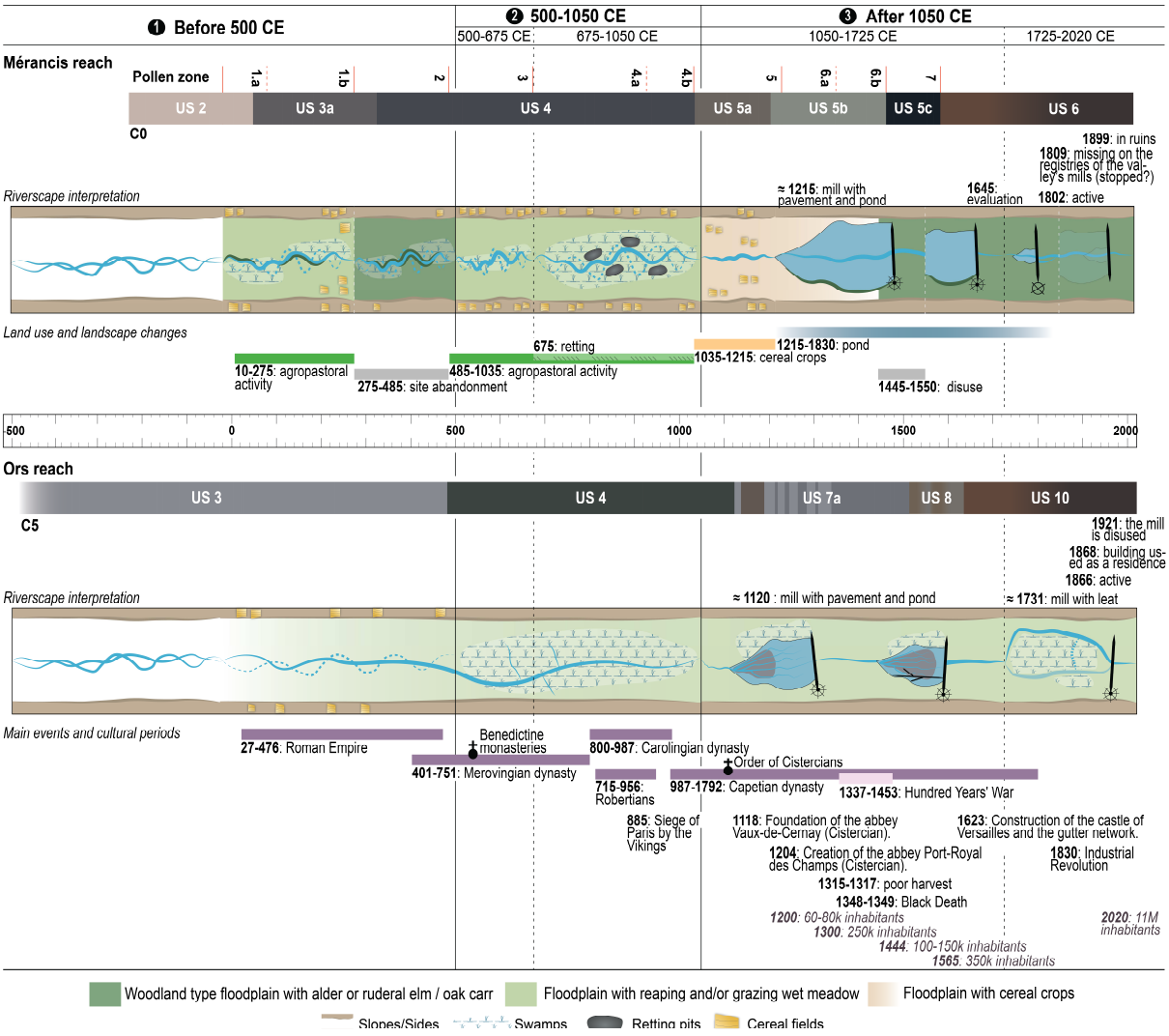

Abstract

This article assesses the long-term hydro-sedimentary and ecological consequences of the urban pressure around Paris over the last 3,000 years on the Mérantaise river. Using a geoarchaeological approach combining sedimentological, geochemical, palynological and geophysical investigations enabled us to identify the transformations of the hydrosystem and to discuss the consequences of the different types of pressure and to put the role of biophysical and historical legacies into perspective with respect to contemporary dynamics. Using two study sites, one a former pond (Mérancis), the other a former mill site (Ors mill), nine cores, two auger holes and four trenches dug in the valley floor and two electrical

resistivity tomography (ERT) profiles, it was possible to reconstruct the geometry of the sedimentary deposits. Chronostratigraphy was based on 41 radiocarbon dates and the history of vegetation and anthropogenic activities was reconstructed from 42 pollen samples and non-pollen palynomorphs collected from the former pond site. Despite the expansion of wetlands in the valley bottom, the pollen data revealed strong agropastoral activities and cereal growing in the Iron Age and up until the end of the Middle Ages. For the first time, sedimentological data associated with pollen data revealed hemp retting activities from c. 675 CE. From the Late Middle Ages onwards, water management led to the creation of two ponds to feed water mills. Despite the persistence of wetlands, this study highlights the early onset of anthropogenic modifications and in particular, the start of organic pollution and eutrophication in the Early Middle Ages, attesting to early eutrophication of water quality and aquatic environments resulting from the transformation of agropastoral practices and hydraulic pressure around the largest European city during the last 1,500 years, well before the inset of urban sprawl in the watershed.

Keywords: stream, hydrogeomorphology, wetlands, pollen and NPPs, mill ponds, hemp retting, water quality, periurban area, northwest Europe, Late Holocene

1. Introduction

Changes in the valley bottoms in the plains and plateaus of Western Europe that occurred during the Holocene are increasingly well known. Geomorphological and paleoenvironmental research revealed the development of (i) mostly authigenic sedimentation during the Middle Holocene and (ii) from the end of the Iron Age on, destabilization of the slopes, which led to the progressive silting of the valley bottoms by overbank silt. These stages correspond to the progressive shift in the dominance of climatic over anthropogenic forcing in the functioning

of fluvial systems (e.g., Brown et al., 2018; Lespez et al., 2015; Notebaert et al., 2018). Research conducted in the Paris Basin has informed the construction of these stages with numerous studies (e.g., Antoine et al., 2000; Beauchamp et al., 2017; Chaussé et al., 2008; Granai and Limondin-Lozouet, 2014; Le Jeune et al., 2012; Lespez et al., 2015, 2008; Orth et al., 2004; Pastre, 2018; Pastre et al., 2006, 2002). Regional and local disparities in Europe are due to the high spatial variability of morphosedimentary responses to climatic forcing and to the impact of the different environmental management practices implemented by successive societies during the late Holocene (Broothaerts et al., 2014; Brown et al., 2018; Houben et al., 2013; Notebaert et al., 2018).

Beyond this general framework, studies of the impact of hydraulic developments on small hydrosystems are less numerous. Although the consequences of building small dams and weirs are now increasingly better known (e.g., Csiki and Rhoads, 2010; Skalak et al., 2009), studies of the long-term consequences of these structures are still rare in Europe (Downward and Skinner, 2005; Kalicki et al., 2020; Maaß et al., 2019; Poeppl et al., 2015), whereas in northeastern America, such studies are more systematic (e.g., Donovan et al., 2016, 2015; Dow et al., 2020; Merritts et al., 2013, 2011; Schenk and Hupp, 2009; Walter and Merritts, 2008). Nevertheless, the focus is more often on the hydro-sedimentary consequences for current systems than their impacts on the fluvial systems during the centuries in which they operated. The forced sedimentation upstream of the hydraulic structures is often highlighted whereas the chronology and nature of sedimentary transformations caused by the creation of reservoirs and the leats and their hydro-sedimentary management remain poorly studied (Beauchamp et al., 2017; Dow et al., 2020) and their ecological impact remains to be documented (Inamdar et al., 2021). From this point of view, the weight of long-term urban pressure on the dynamics of river systems is a major issue. Indeed, historical and geohistorical research has revealed the increasing impact of urban demand on the growing hydraulic

89 pressure in Europe (Brown, 1997; Mauch & Zeller, 2008), and in France (Guillerme, 1983;
90 Frioux et al., 2010). In the Paris region, the impacts of mills on small rivers are evidence for
91 the influence of urban growth on the increase in hydraulic pressure since the Middle Ages,
92 sometimes far from urban centres (Benoit, 2000; Benoit et al., 2003; Berthier, 2007;
93 Dmitrieva et al., 2018; Jugie et al., 2017; Le Roux, 2010; Rouillard et al., 2011) . Indeed, in
94 the medieval period, Paris was by far the largest city in Europe and its population tripled from
95 60,000 to 80,000 inhabitants in 1200, to 250,000 a century later (Bourlet and Layec, 2013).
96 The city depended on agricultural products for its survival and, as J.-M. Moriceau (1994)
97 stated, “Paris ate its nearby countryside”. The demand for power and food resources has
98 affected the entire river system, especially the 1st to 3rd order in Strahler's classification, as
99 shown by historical research (Benoit et al., 2003). Then, the impact of urbanisation in the 20th
100 and 21st centuries as stream straightening and the imperviousness of catchment areas are now
101 increasingly studied and understood (e.g. Chin, 2006; Jugie et al., 2018; de Milleville et al.,
102 2022). However, paleoenvironmental research on the consequences of hydraulic structures
103 and the impact of urbanisation remains in its infancy, especially in the case of small rivers of
104 order 1 to 3, which comprise most of the hydrographic network of many cities, 75% in Paris
105 region.

106 The aim of the present study was to assess the hydro-sedimentary and ecological
107 consequences of the transformation of watersheds by agropastoral practices and hydraulic
108 developments of small sub-urban rivers over time. The Mérantaise River offers an opportunity
109 to examine the environmental history of a small river that has been an integral part of the
110 metabolism of Paris since medieval times. Our specific objective was to identify the
111 transformations of the hydrosystem over the last three millennia and to discuss the
112 consequences of the different types of pressure to put the role of biophysical and historical
113 legacies into perspective with respect to contemporary dynamics.

2. Field study and previous studies

The 13.4 km long Mérantaise River, a tributary of the Yvette, which itself is a tributary of the Seine, is in the southwestern part of the Paris region (Fig. 1A, B). Its natural topographic basin measures 32 km², but with the increase in impervious surfaces and the management of stormwater, the hydrographic basin now covers 36 km² (Jugie et al., 2018) (Fig. 1A, B).

Fig. 1. Location of the study site.

A: Regional location and changes in the urban area over recent centuries; B: location of the Mérantaise watershed (Ws); C: longitudinal profile coupled with geology (BRGM). Changes to urban areas were identified using the following maps (Institut Paris Region): XVIIIth - "carte des Chasses du Roi" (King's hunting map, 1764-1807); XIXth - topographic map type 1900; XXth - from IGN aerial photographs (1949 & 2017).

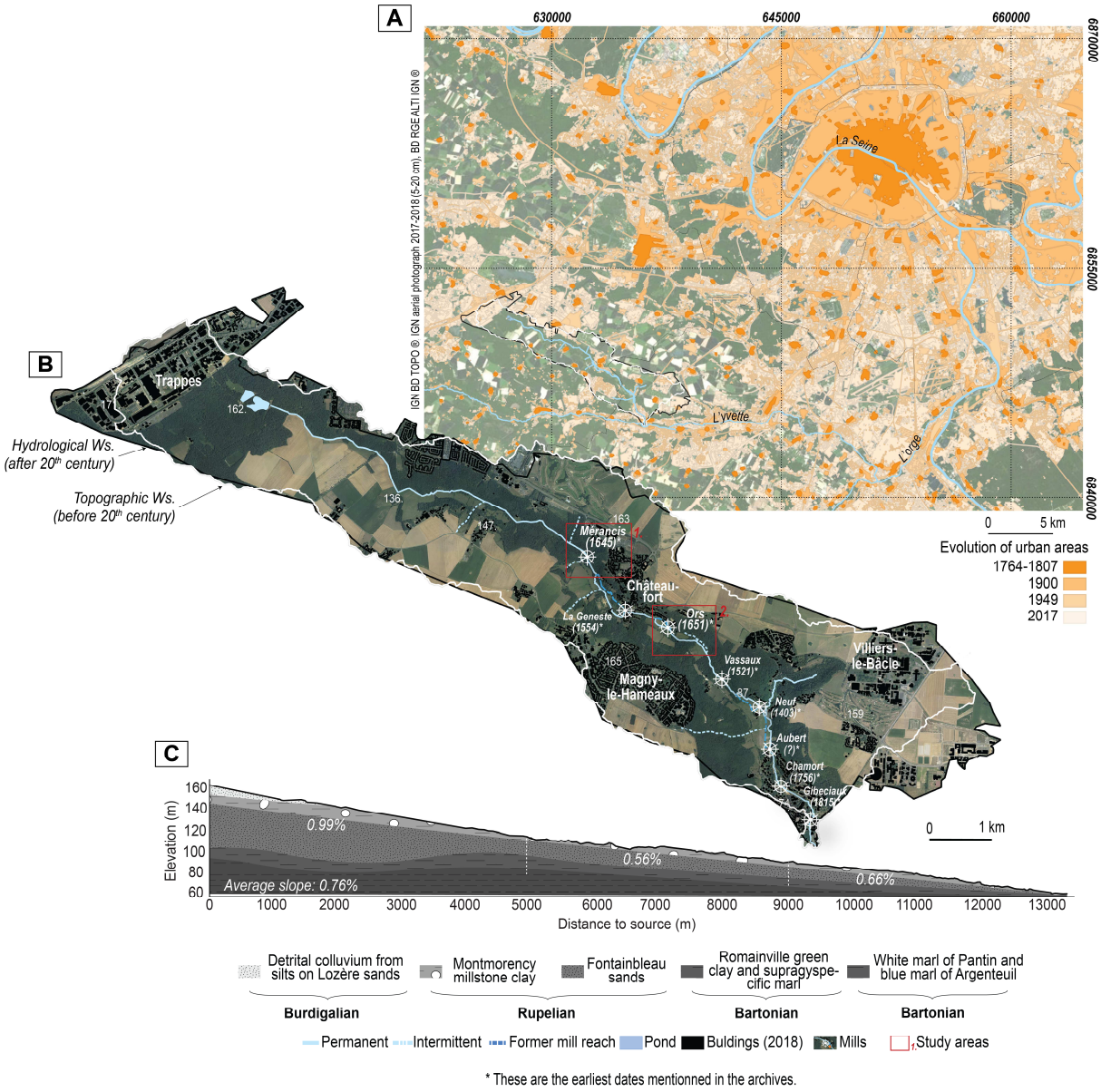

2.1. Morphological and hydrological characteristics of the Mérantaise river basin

The Mérantaise river has a moderate slope (0.76%) (Fig. 1C) and an average width of just over 4 m. Its river basin is largely covered by loess silts. The river is gradually incised into the Tertiary bedrock that is characteristic of the central Paris Basin. Upstream, the plateaus are covered by Lozère sands (Burdigalian), frequently mixed with Pleistocene loess silts due to colluvial processes. These are clayey sands with quartz grains, coarse and poorly classified (0.4-2 mm). Their mineralogy is characterised by low feldspar content (< 5%), high iron hydroxide content (72-77%) and by an association of heavy minerals composed notably of

zircon (20%) and rutile (7%) (Larue and Etienne, 2000). The valley then cuts into the ferruginous millstone clays of Montmorency (Upper Rupelian), and then into white or yellowish nodular marly limestone (Étampe limestone, Upper Rupelian). The valley next incises the Fontainebleau sands (Upper Rupelian) which are the most developed formation of the geological bedrock and reach a thickness of 65-70 m. These are fine sands (median 0.15 mm), yellowish white, well sorted, siliceous (97-99% silica). Their mineralogical signatures can be distinguished from Lozère sands by their high tourmaline content (60%) and low zircon (3.5%) and rutile (2.5%) contents (Larue and Etienne, 2000). Finally, over its last few kilometres, the Mérantaise river flows over the impermeable green clays of the Lower Rupelian (Fig. 1C). The bottom of the river bed is mostly sandy gravels (D_{50} and D_{84} are respectively on average 26 and 52 mm, Table 1), although clay slabs are very frequently exposed.

The hydrological regime of the Mérantaise river is of the rainfall-evaporation type. It is influenced by the degraded oceanic climate of the central Paris Basin but also by urbanisation of the watershed (Jugie et al., 2018). The average annual precipitation is 706.7 mm. Intense floods following thunderstorms occur regularly in summer, but high water usually occurs in winter, between December and March, while low water usually occurs in late summer, between August and September. The mean annual discharge of the Mérantaise at Châteaufort (58% of the watershed) is 0.1 $m^3.s^{-1}$, i.e., a specific discharge of 4.9 $l.s^{-1}.km^2$. Over a period of nine years (2012-2021), the maximum discharge recorded was 4.0 $m^3.s^{-1}$ in 2016 while the minimum flow recorded was 0.01 $m^3.s^{-1}$. The Mérantaise is a low energy river, its specific power calculated at Châteaufort is 16.0 $W.m^{-2}$ (Table 1).

Table 1. Main characteristics of the Mérantaise basin.

Flow measurements recorded at 15-minute intervals were taken from a 9-year series (2012–2021) at a station draining 58% of the whole catchment (i.e., 20.4 km²). The bankfull discharge was determined from the classified flows (flow not exceeded 99% of the time).

Watershed characteristics	
Watershed topographic (km²)	32
Watershed hydrologic (km²)	36
Linear (km)	13.4
Total impervious area (%)	24.3
Parks and gardens areas (%)	11.7
Agricultural area (%)	36.7
Forest area (%)	27.3
Average morphological characteristics	
Mean bankfull width (m)	4.6
Mean bankfull depth (m)	1.5
Mean ratio W/D (m)	3.5
Thalweg slope (m/m)	0.0076
D_{50} (mm)	26
D_{84} (mm)	52
Hydrological characteristics at the mill of Ors station (20.4 km²)	
Mean annual discharge (m^3/s)	0.1
Mean annual specific discharge (l/s/km²)	4.9
Bankfull discharge (m^3/s)	0.6
Specific stream power (W/m²)	16.0
Observe maximal discharge (m^3/s)	4.0

2.2. History of hydraulic works and urbanisation over the last four centuries

Previous studies report the existence of many different types of infrastructure (mills, dams, diversion sluices, laundry washing sites and channelized reaches of the river) that played roles in the morphological and hydrological modification of the Mérantaise river for centuries (Fig. 2). Three major series of recent changes were identified by Jugie et al. (2018): (i) Between the 17th and the end of the 19th century, the Mérantaise river was used to produce hydraulic power. At the time, the valley comprised 74% agricultural land and 24% forest; the channel was more than 80% artificial, including 50% diverted and 30% rectified (Fig. 2). (ii) Between 1880 and 1950, the Industrial Revolution saw the gradual dismantling of the hydraulic infrastructures (Fig. 2). Six out of eight mills were abandoned and the remaining two were

converted into a hydroelectric plant(Jugie et al., 2017). (iii) Between 1949 and 2017, massive urbanisation was underway, and the percentage of urbanised area increased sixfold (from 4% to 24%). This led to major hydromorphological modifications and the bed of the Mérantaise is now incised and eroded in many places (Fig. 2), like many small rivers in peri-urban contexts (Chin, 2006; Walsh et al., 2015).

Fig. 2. Hydraulic developments and urbanisation over the last centuries (modified after Jugie (2018)).

Changes in land use were identified using the following maps: XVIIIth - "carte des Chasses du Roi" (King's hunting map, 1764-1807); XIXth - topographic map 1900; XXth - IGN aerial photographs (1949 & 2017). The values in m indicate the distance between each mill.

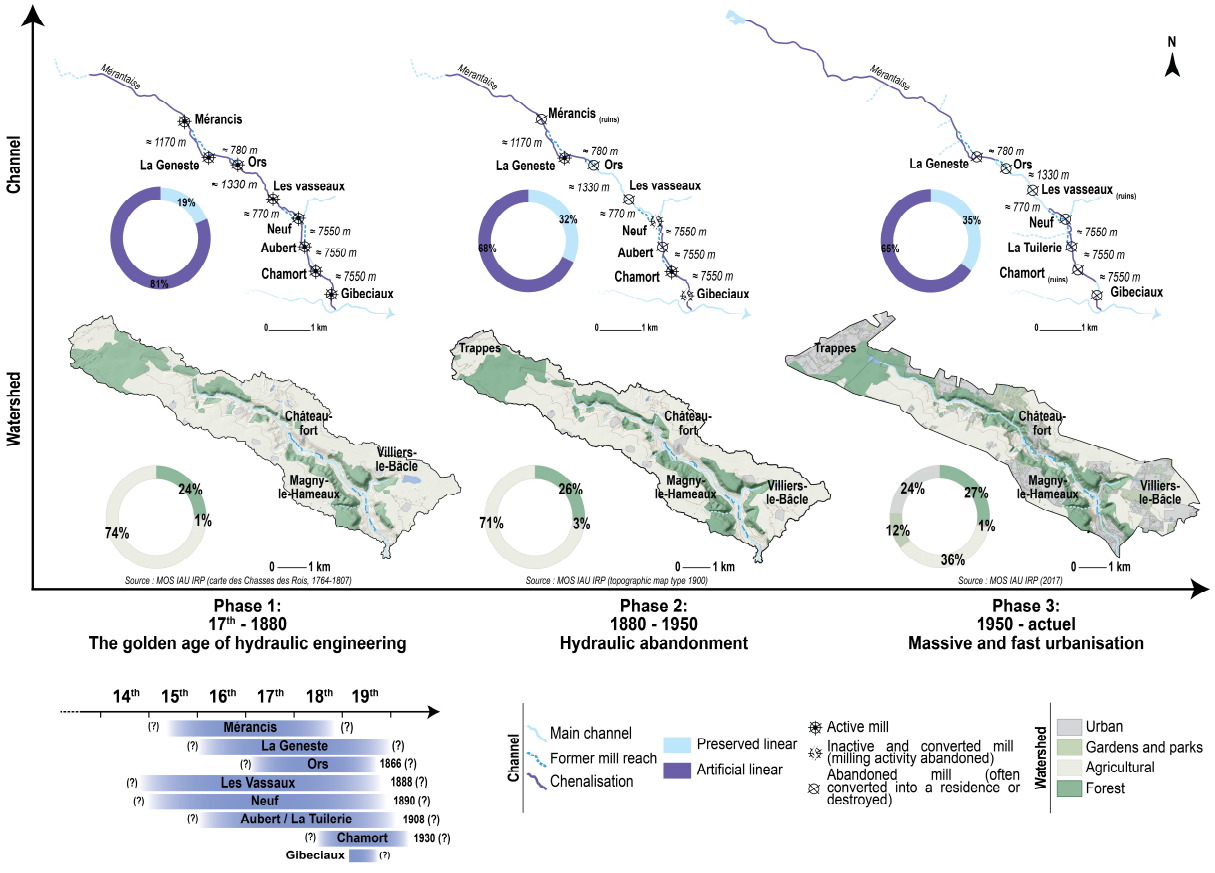

2.3. History of Mérancis pond and Ors mill

Two sites were chosen to analyse the impact of valley management and watershed transformation on the functioning of the Mérantaise river. The first site is a former pond, Mérancis pond, which offers the opportunity for paleoenvironmental studies (Fig. 3). Until the end of the Hundred Years War, the Mérancis valley bottom contained six ponds (Tulippe, 1934; Stephan, 2007). Two of the ponds became pastures and/or woods, the remaining four were restored in 1521. Mérancis mill was installed on one of the two ponds. A description of the domain reports its functioning until 1802. A century later (1899), in the municipal monograph of Magny-les-Hameaux, the mill of Mérancis was reported to be "completely in ruins". The pond and the mill were last mapped on the État-major map (1818-1835) (Fig. 3). Today, all that remains is the causeway that blocked the entire valley floor to build a reservoir to supply the mill. Today, the former pond is a marsh colonised by shrubby vegetation composed of alder, maple and ash, as well as herbaceous and helophytes plants, while the Mérantaise flows in a straight channel bordered by a few hazel trees.

Fig. 3. Study area 1: the former Mérancis pond.

The names of the maps have been translated into English. The original references are a. Carte de l'abbé Delagrive *(1731-1741); b.* Carte des chasses du Roi *(1764-1807); c.* Plan de la paroisse de Magny-les-Hameaux *(1790); d.* Carte d'État-major *(1818-1835).*

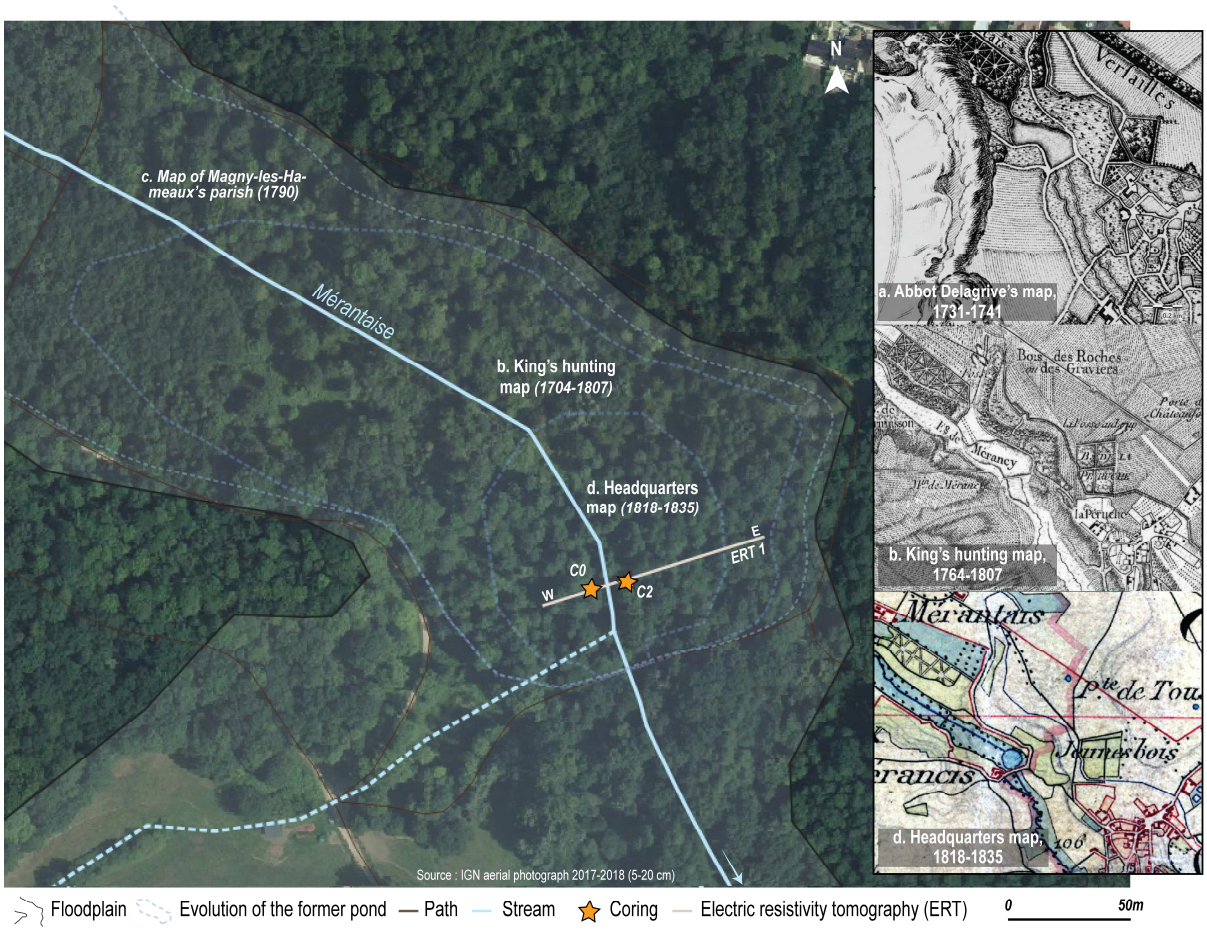

207

208

209 The second site is located 2 km downstream and corresponds to the reach preceding Ors mill
210 (Fig. 4). This site enabled characterisation of changes in the channel before and after the
211 construction of the waterworks. Ors mill is mentioned for the first time in 1651 in a tenancy
212 agreement (Stephan, 2007) and is attached to the estate that belonged to the powerful
213 seigneury of Châteaufort (Jugie et al., 2017). It is characteristic of bypass mills, fed by a leat
214 (perched reach) while the main channel is called "morte rivière" (dead river). It was used as a
215 grist (flour)mill until 1866. The mill then fell into disuse, the millstream was abandoned and
216 the "morte rivière" put back under water. The Mérantaise is bordered by a riparian zone with
217 alder trees, and the alluvial plain is a wetland mainly composed of helophytic plants (e.g.,
218 sedges, common reed, bur-reed, mint).

219

Fig. 4. Study area 2: Ors mill.

The names of the maps have been translated into English. The original references are a. Carte de l'abbé Delagrive *(1731-1741); b.* Carte des chasses du Roi *(1764-1807); d.* Carte d'État-major *(1818-1835).*

3. Materials and Methods

3.1. Reconstruction of the sedimentary architecture of the alluvial plain

The alluvial fill geometry was first analysed by geophysical prospecting. Several electrical resistivity tomography (ERT) profiles were carried out using an Abem Terrameter LS system composed of 64 electrodes. At the site of the former Mérancis pond, a 94 m long west-east transverse profile was made of the valley (Fig. 3). The east-west profile of Ors mill is 167 m long (Fig. 4). With an inter-electrode spacing of one metre and a Wenner-Schlumberger type electrode configuration, the investigation reached a depth of six metres. The topography of the profiles was surveyed using differential GPS (Trimble Geoexplorer). Data processing was performed with Res2Dinv software (Loke and Barker, 1996) using the least squares inversion method (Milsom, 2011; Reynolds, 2011). Between three and five iterations were required to

obtain a root mean square error of less than 5% between the measured and calculated profile. For better comparison, both ERT profiles were brought to the same value. At the Mérancis site, the range of values varies between 7.43 and 99.7 ohm.m, while at the Ors mill site the values are higher, up to 154 ohm.m. This difference can be explained by the greater presence of coarse sand and the presence of large millstone blocks, which are not found upstream, i.e., at Mérancis. The ERT profiles allow the identification of large sedimentary units with a metric resolution due to the measurement protocol used, but only coring and trench, which allow a fine description of the sediments, allow a resolution of the order of a centimetre. These geophysical profiles were then used to identify the position of the cores needed to reconstruct the architecture of the alluvial plain and the succession of sedimentary facies. A total of nine cores, two auger holes, and four trenches were completed in the valley floor between October 2017 and September 2020 (Table 2). The nine 50-mm diameter cores were drilled to a depth of six metres using a percussion corer (Cobra TT) (Table 2). The nature of the sediments was described and interpreted using standard methods of description in a fluvial context (Brown, 1997). Analyses were performed on two cores, one at each site, hereafter called reference cores C0_MER and C5_MDO (Table 2).

Table 2. Location of the field operations and summary of the analyses

*The two cores and the reference trench are shown in blue. The numbers represent the number of samples analysed. *MS: Magnetic susceptibility. The analyses marked with the following symbol ✓were performed.*

Study area	Coring reference	Depth (m)	Location (Lambert 93)			Dating C^{14}	Granulo-metry	*MS	X-ray fluorescence	Pollens and NPP's
			X	Y	Z					
Mérancis pond	C0_MER	6	632507.01	6849231.482	107.75	**8**	**74**	✓	✓	**42**
	C2_MER	6	632530.248	6849245.05	107.89	**4**	×	✓	×	×
The mill of Ors	C0_MDO	3	633732.823	6848131.124	96.69	×	×	×	×	×
	C12017_MDO	2	633736.128	6848137.865	96.64	**2**	**20**	✓	×	×
	C1_MDO	4	633727.277	6848123.699	96.76	**4**	×	×	×	×
	C2_MDO	4	633715.422	6848111.603	96.72	**5**	**78**	✓	✓	×
	C3_MDO	2	633711.918	6848093.456	96.73	×	**46**	×	×	×
	C4_MDO	5	633712.8	6848096.202	96.73	**5**	**63**	✓	×	×

C5_MDO	5	633719.23	6848119.241	96.86	**7**	**79**	✓	✓	×
S3_MDO	1.52	633743.156	6848152.201	97.00	×	×	×	×	×
S2_MDO	2	633737.695	6848141.061	96.76	×	×	×	×	×
Trench 1	1.75	633712.665	6848097.207	/	**3**	**3**	×	×	×
Trench 2	1.3	633712.851	6848083.685	/	×	**1**	×	×	×
Trench 3	1.7	633715.042	6848113.575	/	×	×	×	×	×
Trench 4	1.75	633709.238	6848101.479	/	**3**	**3**	×	×	×

3.2. C^{14} Dating

The chronology of the fluvial deposits is based on 41 radiocarbon dates obtained at the two study sites (Table 3). Dating was performed using the AMS method at the Poznan laboratory, Beta Analytic and Direct AMS. Radiocarbon ages were calibrated using OxCal v4.4 software (Bronk Ramsey, 2017) based on the IntCal20 atmospheric curve (Reimer et al., 2020). From the 41 dates obtained from the two cores, two age-depth models were created using the Bayesian model in the Bacon package in R (Blaauw and Christen, 2011, version 2.5.7).

Table 3. Radiocarbon dates

(*) indicates where the date is probably too old or too young and may have been reworked.

Lab number	Sample reference	Depth (cm)	NGF (m)	Material	BP	Cal BCE-CE (cal 2σ - IntCal 2020)	Cal yr. BP (cal 2σ - IntCal 2020)
Poz-118582	C0.1 MER	83.8-85	106.93	Organic sediment	1095 ± 30 BP *	890-1017 cal CE	1060-934 cal BP
Poz-135359	C0.1 MER	86.3-87.5	106.88	Organic sediment	800 ± 30 BP	1180-1279 cal CE	770-672 cal BP
Poz-118573	C0.3 MER	253.8	105.21	Organic sediment	1050 ± 30 BP	895-1035 cal CE	1055-916 cal BP
Poz-135360	C0.3 MER	300.0	104.75	Organic sediment	1200 ± 30 BP	706-945 cal CE	1244-1006 cal BP
Poz-118575	C0.4 MER	390.6	103.85	Twig	3900 ± 35 BP *	2471-2236 cal BCE	4420-4185 cal BP
Poz-118576	C0.5 MER	416.9	103.58	Twig	2000 ± 30 BP	51 cal BCE-116 cal CE	2000-1835 cal BP
Poz-118333	C0.5 MER	460.2	103.15	Twig	2000 ± 30 BP	51 cal BCE-116 cal CE	2000-1835 cal BP
Poz-118332	C0.5 MER	488.0	108.87	Twig	2035 ± 30 BP	149 cal BCE-65 cal CE	2098-1886 cal BP
Poz-135361	C2.1. MER	27.6	107.61	Charcoal	115 ± 30 BP	1680-1940 cal CE	270-10 cal BP
Poz-135374	C2.2. MER	145	106.44	Organic sediment	1100 ± 30 BP	887-1017 cal CE	1064-934 cal BP
Poz-135375	C2.4. MER	384	104.05	Organic sediment	1740 ± 35 BP *	244-403 cal CE	1707-1547 cal BP
Poz-135376	C2.5. MER	499	103.00	Organic sediment	3165 ± 30 BP	1503-1326 cal BCE	3452-3275 cal BP
Beta - 490195	C1.1 MDO2017	60	96.04	Twig	590 ± 30 BP	1302-1412 cal CE	648-538 cal BP
Beta - 490194	C1.2 MDO2017	198	94.66	Gyttja	2030 ± 30 BP	147 cal BCE-69 cal CE	2096-1882 cal BP
Poz-118595	C1.2 MDO	116	95.6	Twig	870 ± 30 BP	1047-1261 cal CE	903-689 cal BP
Poz-118579	C1.2 MDO	162	95.14	Peat	995 ± 30 BP	992-1154 cal CE	958-796 cal BP
D-AMS 033823	C1.3 MDO	225	94.51	Organic sediment	1591 ± 28 BP	420-545 cal CE	1531-1405 cal BP
D-AMS 033824	C1.4 MDO	313	93.63	Twig *(cf. Ericaceae)*	1704 ± 28 BP *	255-416 cal CE	1696-1534 cal BP
Poz-118596	C2.2 MDO	133	95.39	Twig	1720 ± 30 BP	250-411 cal CE	1700-1539 cal BP

Poz-118334	C2.2 MDO	189	94.83	Twig	1010 ± 30 BP	990-1154 cal CE	960-797 cal BP
Poz-118578	C2.3 MDO	294	93.78	Charcoal	2015 ± 30 BP	95 cal BCE-109 cal CE	2044-1841 cal BP
D-AMS 033825	C2.4 MDO	307	93.65	Twig	1717 ± 27 BP	251-412 cal CE	1700-1538 cal BP
D-AMS 033826	C2.4 MDO	368	89.04	Twig	4423 ± 31 BP *	3326-2920 cal BCE	5275-4869 cal BP
Poz-118594	C4.1 MDO	26	96.47	Charcoal	785 ± 30 BP	1218-1280 cal CE	733-671 cal BP
Poz-118583	C4.1 MDO	68-71	96.10	Twig	890 ± 60 BP	1032-1261 cal CE	918-690 cal BP
Poz-118585	C4.2 MDO	135	95.38	Twig	825 ± 30 BP	1170-1270 cal CE	780-680 cal BP
Poz-118331	C4.2 MDO	178	94.95	Twig	890 ± 30 BP	1045-1223 cal CE	906-728 cal BP
Poz-118586	C4.3 MDO	268	94.05	Twig	1040 ± 30 BP	896-1114 cal CE	1055-836 cal BP
Poz-118587	C5.2 MDO	118-120	95.67	Twig	350 ± 30 BP	1461-1636 cal CE	489-315 cal BP
Poz-118580	C5.2 MDO	163.5-164	95.22	Organic sediment	860 ± 30 BP	1052-1263 cal CE	898-688 cal BP
Poz-118581	C5.2 MDO	198.5-199	94.87	Peat	1115 ± 30 BP	775-1014 cal CE	1176-937 cal BP
Poz-118588	C5.3 MDO	261.4	94.25	Twig	1995 ± 30 BP	48 cal BCE-116 cal CE	1997-1835 cal BP
Poz-118589	C5.4 MDO	327.6-328.1	93.58	Twig	1745 ± 30 BP *	242-401 cal CE	1708-1549 cal BP
Poz-118590	C5.4 MDO	370	93.16	Twig	2095 ± 30 BP	197 cal BCE-1 cal CE	2146-1949 cal BP
Poz-118591	C5.5 MDO	431	92.55	Twig	2505 ± 30 BP	780-540 cal BCE	2729-2489 cal BP
Poz-135352	T1 log1	75	95.97	Twig	815 ± 30 BP	1175-1275 cal CE	775-675 cal BP
Poz-134381	T1 log2	103	95.70	Organic sediment	785 ± 30 BP	1218-1280 cal CE	733-671 cal BP
Poz-135354	T1 log6	80	95.97	Organic sediment	765 ± 30 BP	1222-1284 cal CE	729-667 cal BP
Poz-135355	T4 log11	50	96.3	Organic sediment	700 ± 30 BP	1267-1388 cal CE	683-563 cal BP
Poz-135356	T4 log11	74	96.06	Organic sediment	790 ± 30 BP	1215-1280 cal CE	736-670 cal BP
Poz-135358	T4 log11	120	95.60	Organic sediment	850 ± 30 BP	1054-1267 cal CE	896-684 cal BP

Fig. 5. Age-depth model of the C0 and C5 cores

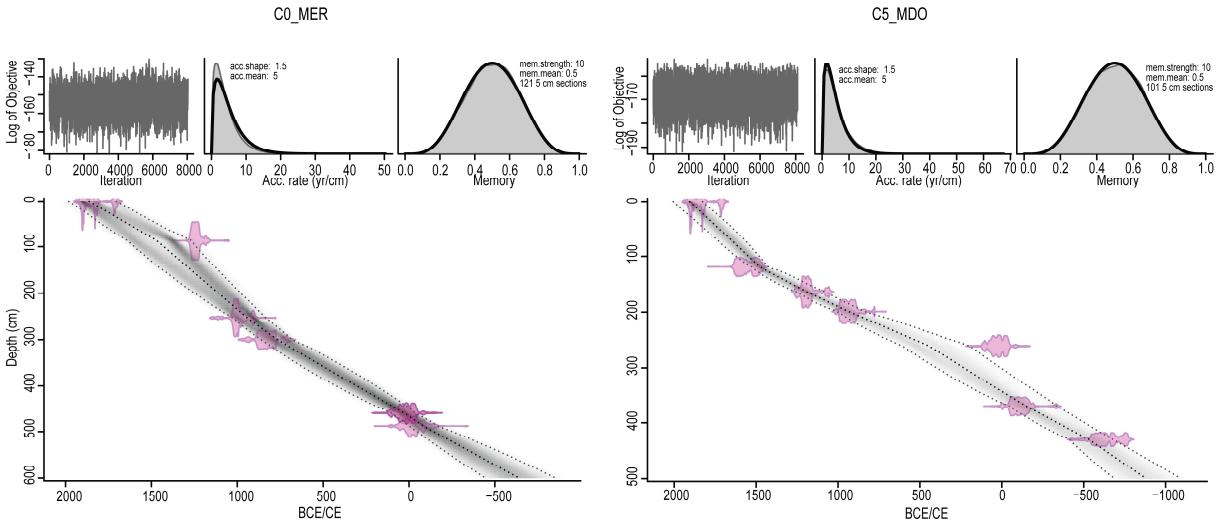

3.3. Sedimentological analyses

According to the defined sedimentary units, 360 samples were taken from the six cores, and seven samples were taken from the base of the paleochannels identified in trenches T1, T2 and T4 (Table 2). For grain size analyses, organic matter was removed with 35% hydrogen

peroxide and particle dispersion was performed by stirring in a 5 ‰ sodium hexametaphosphate solution. Grains from 0.04 to 2000 µm in size were measured by laser diffraction using a Beckman Coulter LS230. Coarse grains (more than two millimetres in size) were isolated using sieves with mesh sizes ranging from two to eight millimetres, and particles more than eight millimetres in size were measured on the b-axis. The results were analysed using GRADISTAT (Blott and Pye, 2001; version 9.1).

3.4. Magnetic susceptibility

The presence of magnetic minerals in sediments may be due to the lithology of the watershed, to the remobilisation of surface sediments, to their physical characteristics (size, shape, nature) and to deposition processes (Dearing et al., 1996). Magnetic susceptibility (MS) was measured to look for evidence of pedogenesis, redox phases, organic matter accumulation, or magnetic mineral-enriched detrital phases (Dearing et al., 1996; Verosub and Roberts, 1995). Volume MS (expressed as χvol. x 10-5 SI) was measured with a Bartington Susceptibility Meter MS2F probe at 0.5 cm intervals in a double pass (Table 2). Values were averaged and then multiplied by two to correct for the effect of the probe used.

3.5.Geochemical analyses

The high frequency X-ray fluorescence spectrometry (XRF) method (0.5 cm sampling step) was used to estimate the relative concentration of major elements at the surface of the reference cores (Table 2). Analyses were performed using an ITRAX scanner (Cox analytical systems). The uncalibrated values of the identified elements (Ti, K, Rb, Zr, Si, Fe, Mn, Ca, Sr, Inc/Coh) are expressed in counts per second (cps) (Supplementary data S1). The silicon (Si) signal was always poor in both reference cores. The titanium (Ti) signal was used to identify terrigenous detrital inputs, and hence erosive processes in the watershed, because it is a stable

signal that is not affected by weathering or redox processes (Arnaud et al., 2012; Lu et al., 2017). The calcium (Ca) signal was used to identify carbonate inputs. As these can be of terrigenous or authigenic origin, the Ca/Ti ratio was used to distinguish them. The iron (Fe) signal was analysed to identify potential variations in redox conditions, and the Fe/Ti ratio was calculated to distinguish detrital sources (Davison, 1993; Kylander et al., 2011). Values were then compared to the mean to identify a relative increase or decrease.

3.6.Pollen and Non-Pollen Palynomorphs (NPPs)

The palynological study was performed on 42 samples taken from the C0_MER borehole at 10-cm intervals between a depth of 65 cm and 456 cm. With respect to the established age-depth model, the pollen sequence begins at c. 13 CE and ends at c. 1550 CE. The average temporal resolution was estimated to be 37 years per pollen spectrum (minimum 18 years, maximum 87 years). For the analysis of pollen and NPPs (algae, fungal remains, microfossils, other unidentified palynomorphs), the same standard protocol applied to 1.5 to 2 grams of sediment involved sieving to 200 µm, KOH 10% hot, densimetric separation (SPT density 1.9). Pollen grains were identified using pollen keys, pollen atlases (Moore et al., 1991; Beug, 2004; Reille, 1992, 1995, 1998) and the pollen collection of the Physical Geography Laboratory. Identification of NPPs was based mainly on van Geel (1978, 2001), van Geel and Aptroot (2006), Gelorini (2011), Cugny (2011) and the Non-Pollen Palynomorph Image Database (NPP-ID, Shumilovskikh et al., 2021).

Counts were made until a pollen sum of at least 400 grains (pteridophyte spores, indeterminate pollen grains and NPPs excluded) was obtained, 150 of which were outside the dominant taxon, and at least 20 pollen taxa. The NPPs were counted in parallel with the pollen counts on the same microscope slides. Concentrations were calculated using the volumetric method (Cour, 1974). Pollen percentages were calculated from a sum excluding

pteridophyte spores, indeterminate pollen grains and NPPs. Percentages of pteridophyte spores and indeterminable grains were calculated by including them in the sum. NPPs are expressed as concentrations (grains/gram of sediment). The results are presented in four diagrams constructed with the Psimpoll software (http://www.chrono.qub.ac.uk/psimpoll/psimpoll.html): pollen percentages (Fig. 8 and Supplementary data S3A, B), pollen concentrations (Supplementary data S2), algal concentrations (Supplementary data S4, S5) and fungal spores and other NPPs concentrations (Fig. 9 and Supplementary data S6, and S7A, B). Seven local pollen zones were identified based on the definition of Gordon & Birks (1972) and Birks & Birks (1980). This zonation is consistent with the one defined using the CONISS function. Pollen zonation was applied to the algal, fungal spores and other NPPs concentrations diagrams.

4. Results

The descriptions of the sedimentary environments are based on all the cores, boreholes and trenches at the two study sites, whereas the sedimentological and geochemical analyses are based only on the two reference cores, C0_MER (Mérancis) and C5_MDO (Ors mill). The sedimentary units are described according to their depth and for each, the time frame of the filling taken from the age-depth models is indicated (Fig. 5).

4.1. The former Mérancis pond

4.1.1. Sedimentary architecture, sedimentology, and geochemistry

Comparing the resistivity value with the sedimentary facies present in the two cores provided an initial reading of the sedimentary fill architecture (Fig. 6). Resistivity values ranged from 7.43 to 64 Ωm. Values ≥ 42 Ωm corresponding to silty-sandy sediment concentrated at the base of the profile over three to four metres in depth. Values between 42

and 27.2 Ωm indicate coarse silts. The lowest values (≤ 27.2 Ωm) correspond to an organic-rich medium silt sediment developing over one to two metres in depth. The analyses performed are documented in Figure 7.

Fig. 6: Architecture and sedimentary filling of the former Mérancis pond.

A: Cross-sectional profile of electrical resistivity tomography, C0 and C2 coring, and ^{14}C dating; B: Description of the six sedimentary units.

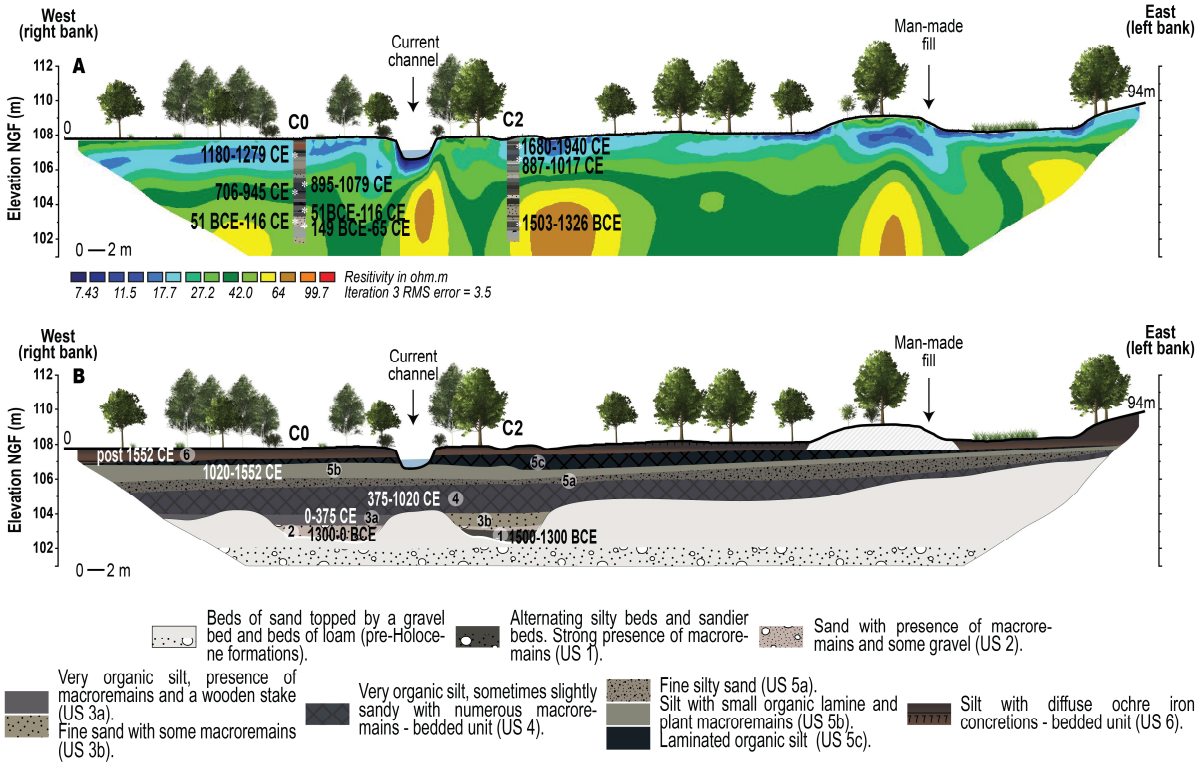

Pre-Holocene Formations

Fine to medium ochre sand beds with a gravel bed and grey-beige, slightly sandy silty beds were observed at the base of both cores (C0 and C2). The MS was low (6-7 x 10^{-5} SI), and the Si content generally high. Ti content was initially low and reached 2,000-3,131 cps before following a similar pattern to Fe. Manganese (Mn) and calcium (Ca) signals, as well as Ca/Ti and Inc/Coh ratios were low. These form the local substrate, which features mainly Fontainebleau sands, which may have been reworked by erosive processes.

Unit 1 (c. 3500-3250 cal BP; 1500-1300 BCE)

This unit was only identified in core C2. The base comprised medium to coarse light gray sand with gravels in an approximately 15-cm thick layer, followed by alternating highly organic black-brown silty beds with numerous macroremains and slightly sandier beds (38 cm thick). The ensemble was topped by a new 18-cm thick peaty bed, the top of which was dated to 1503-1326 BCE. This is the first Holocene fluvio-palustrine deposit to show aggradation in the valley bottom.

Unit 2 (c. 3275-1950 cal BP; 1300 BCE-0 CE)

This unit is clastic. The base was made of a coarse bed consisting of multi-centimetric pebbles in a beige silty matrix. Sedimentation continued with beige sandy beds with occasional gravels and plant macroremains, and centimetre-thick organic brown silty layers. This unit was less dilated in core C2 (22 cm) than in C0 (66 cm). The MS was low at around -1 x 10^{-5} SI with a slight peak around 10 x 10^{-5} SI. The Si signal was high in the first 40 cm of the unit (C0), but decreased in the last few cm. The Ti signal was below average; the only two peaks found (2,419 and 1,954 cps) at the base and top of the unit corresponded to silty beds. The other elements and ratios (Fe, Fe/Ti, Mn, Ca, Ca/Ti) were constant and homogeneous. The Inc/Coh signal was below average but increased progressively towards the top of the unit, consistent with the more organic facies described above. Two twigs within this unit were dated at 149 BCE-65 CE and 51 BCE-116 CE.

Unit 3 (c. 1950-1575 cal BP; 0-375 CE)

This unit was subdivided into two subunits. Subunit 3a, in C0, was characterised by greyish-brown to dark grey silty facies that were more or less peaty and slightly sandy.

Subunit 3b in C2, appeared to be a lateral evolution of this unit. It was characterised by a light grey fine sand with some plant macroremains and flint fragments and composed of two peaty beds (11 and 2 cm thick). The MS was low and varied between -1 and 7 x 10^{-5} SI. The Ti signal increased whereas the Fe, Ca, and the Fe/Ti and Ca/Ti ratios remained constant. Ochre tile fragments were retrieved at the base of the unit. The base of a peat bed was dated and yielded the same date as the previous unit (51 BCE-116 CE). The assemblage suggests a palustrine environment characterised by silty-sandy fluvial inputs.

Unit 4 (1575-930 cal BP; 375-1020 CE)

This unit was characterised by the development of organic sedimentation in the form of a succession of grey brown to black silty beds with varying peat content and rich in wood fragments. In core C2, the sedimentation is interrupted by a light grey, slightly organic sandy bed between 332 and 352 cm thick. From the base to 328 cm, the MS was low (ranging from -1.7 to 3.1 x 10^{-5} SI). From 328 cm to 281 cm, four peaks greater than 15 x 10^{-5} SI, including one up to 100 x 10^{-5} SI, appeared. MS subsequently decreased; the Si signal was weak (around 163-216 cps). Ti content fluctuated more in this unit. At the base, the relative Ti concentration was low but gradually increased to 325 cm around 2,275 cps and then decreased again to 260 cm around 743 cps to finally stabilise around 1,432 cps. The detrital signal revealed in C0 by the increase in grain size, Ti, and MS is contemporaneous with the sandy bed identified in core C2 thus indicating that the detrital crisis affected the entire valley bottom. The Fe signal remained constant throughout the unit. The Ca signal and Ca/Ti ratio showed an initial phase in which the carbonate concentration remained constant, followed by a sharp increase around 20-25 (Ca/Ti). The Inc/Coh signal fluctuated around the mean (3.93 cps), then increased from 260 cm to 4.88 cps. At the base, a wooden stake about 20 cm long

416 was found embedded in a sandy silty-muddy sediment. Two radiocarbon dates in core C0
417 yielded ages of 706-945 CE and 895-1079 CE.
418
419 **Unit 5 (930-398 cal BP; 1020-1552 CE)**
420 This unit was characterised by clastic sediments. It occupied much of the valley floor and
421 was divided into three successive subunits.
422 Subunit 5a was characterised by a grey-beige silty sand, becoming less sandy towards the top.
423 At the base, the MS was constant around 4-5 x 10^{-5} SI then, from 200 cm, it increased to 12 x
424 10^{-5} SI although with a slight decrease between 186-176 cm. The Ti signal fluctuated
425 significantly within the sub-unit correlated with the silty beds. The Mn signal fluctuated from
426 the base of the unit to 200 cm, then increased towards the top. This increase in Mn appeared
427 to be related to the siltier units. The Ca signal and Ca/Ti ratio indicated an authigenic
428 carbonate peak at the base of the unit. Between 217 and 194 cm, the Ca signal decreased
429 significantly as did the Ca/Ti ratio. From 194 cm onwards, the Ca signal increased again, as
430 did the Ca/Ti ratio, but to a lesser extent. The proportion of terrigenous carbonate was thus
431 higher. Subunit 5b comprised grey-beige silt with small organic laminae and plant
432 macroremains. The MS was high (ranging from 26.2 to 11.2 x 10^{-5} SI) and then, at the top of
433 the unit, decreased to 6.3 x 10^{-5} SI. Two peaks, at 146.5 and 136.5 cm, were correlated with
434 the Fe and Mn peaks. The Fe signal was higher than previously and showed positive
435 fluctuations around the average. This unit was marked by a change in redox conditions,
436 biogenic processes, and oxygenation of the environment. The Si signal was low, below
437 average, while the Ti concentration was high. The Ca signal and the Ca/Ti, Inc/Coh ratios did
438 not vary much indicating an increase in detrital inputs and possibly fluctuating water table
439 levels with drying periods. Subunit 5c comprised dark brown to black laminated organic silt.
440 The MS increased to 22.6 x 10^{-5} SI at 78 cm. All the trace elements analysed showed marked

variations. The low concentrations of Si and Ti imply a reduction in erosive inputs. Conversely, the Fe, Ca, Mn signals and associated ratios (Fe/Ti, Ca/Ti) were high, implying changes in redox processes and in the level of oxygenation of the wetland. The environment became more and more reductive following a rise in the water table level that allowed precipitation of carbonates. The Inc/Coh signal increased relative to the organic matter content of the sediment.

Unit 6 (398-0 cal BP; post 1552 CE)

This unit was characterised by beige-brown to dark brown silt beds with diffuse ochre iron concretions (Fig. 6). The MS increased to constant values around 12-16 x 10^{-5} SI, then decreased at the top to -0.9 x 10^{-5} SI (Fig. 7). The concentration of Si was low but increased from 30 cm onwards to reach a maximum value of 522 cps. The concentration of Ti was high, indicating significant detrital inputs from the catchment area. Fe and the Fe/Ti ratio co-evolved with high concentrations at the base of the unit and decreasing at the top of the unit, from 30 cm, while the concentration of Mn displayed the opposite trend.

Fig. 7: Sedimentological and geochemical analysis of the C0 core.

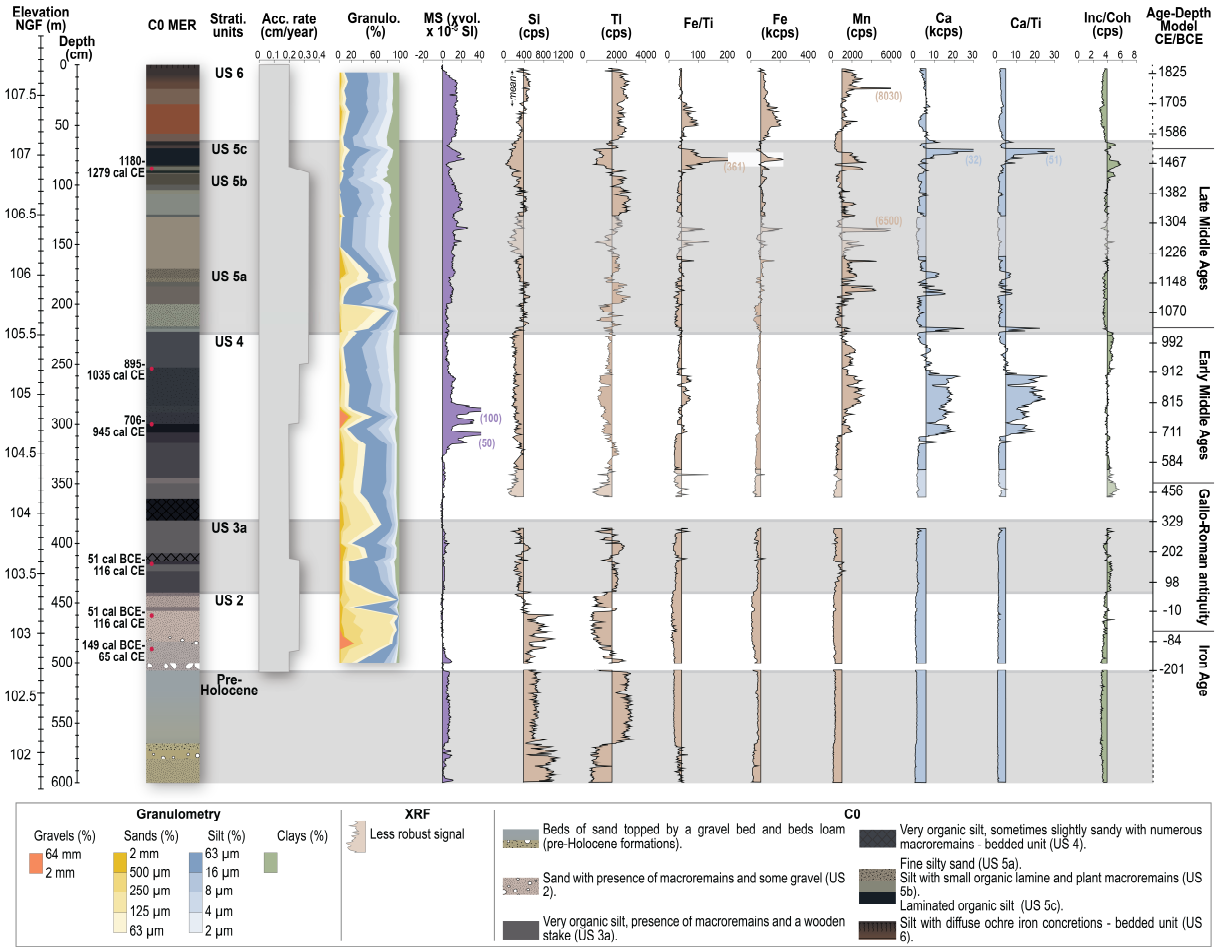

4.1.2. Pollen and Non-Pollen Palynomorphs

Considering that fungal and algal spores only appear in situ (van Geel, 1986), the adequacy of the pollen zonation with, on the one hand, changes in algal assemblages and, on the other hand, in fungal spores and other NPPs assemblages - indicates a mainly local pollen signal. The presence of clusters of the same pollen type (Chenopodiaceae-t., Cichorioideae, *Aster*-t., Cyperaceae, Fabaceae, *Nymphaea*, Poaceae) and/or stomata in 15 samples, as well as the very high diversity of NPPs encountered, confirmed this observation. The diversity of pollen taxa was very high (35-52) and remained relatively constant. At the base of the sequence (Mer-1 to Mer-3 zones), spore and pollen concentrations showed a progressive downward trend, while concentrations of herbaceous pollen were slightly higher than those of arboreal pollen.

469 Concentrations of both fungal spores and microfossils were low. The Mer-4 zone showed
470 both a clear increase in both concentrations of spores and pollen and in fungal spores, with
471 high values, and a more moderate increase in microfossil concentrations. From Mer-5 onward,
472 spore and pollen and fungal spores concentrations decreased sharply but remained higher than
473 those at the base of the sequence. Algal concentrations were extremely low until the Mer-6
474 zone, except in the Mer-4b zone, which had higher values. From the Mer-6 zone on, algal
475 concentrations increased regularly and reached their maximum value in the Mer-7 zone.
476

477 **Table 4. Description of the pollen zones.**

Pollen zone	Description of pollen, algal and NPPs assemblages
Mer-7	**Pollen** Peak of Poaceae (66%) and *Nymphaea* (34%); strong decrease of Cichorioideae (0.3-2%); other stable herbs. Slight increase of Alnus (3-5%), *Betula* (1-6%), *Quercus* (3-17%) et *Castanea* (0.2-3%). **Algae** Maximum concentrations (2,675-132,197gr/g) due to peak of *cf. Debarya* (156-130,682gr/g); small increase of HdV-128, *Mougeotia*; appearance of *Tetraedron* (HdV371) and *Anabaena* (HdV-601). **NPPs** Strong increase in HdV-121 concentrations; small increase in Coniochaetaceae-Xylariaceae, *cf. Scleroderma*, *Melanconis alni* (EMA-3), HdV-181, HdV-731, HdV-187B, *Ceratophyllum* (HdV-137) and HdV-129.
Mer-6	**Pollen** Maximum herbaceous rates (88-93%). Dominance of Poaceae (15-37%) and Cichorioideae (3-14%) although their percentages are decreasing; decreasing values of *Hordeum*-t. (1-5%), *Secale*-t. (0.2-2%), *Triticum*-t. (0.2-4%); stable frequencies of *Plantago lanceolata*-t., *Rumex*, *Polygonum aviculare*-t., Brassicaceae; strong increase but fluctuating values of Cyperaceae (2-32%), *Sparganium emersum*-t. (0.4-7%), *Sparganium erectum*-t. (0.6-14%), *Nymphaea* (2-12%) and *Myriophyllum verticillatum*-t. (0-27%). Minimum of the mean arboreal pollen values (AP 7-12%) due to *Quercus* (~3%), *Corylus* (~2%), *Alnus* (~1%), *Salix* (~1%) and *Betula* (<1%). **Algae** Gradual increase in concentrations (876-28,463gr/g) linked to that of *cf. Debarya* (moy. 8129 gr/g) and to a lesser extent to that of *Botryococcus*, *Spirogyra*, *Rivularia*-t. (HdV-170), *cf. Aphanizomenon*, *Gloeotrichia* (HdV-146) and HdV-128B. **NPPs** Increased concentrations (5,629-13,963gr/g) but no great diversity; strong increase of *Xylomyces* (HdV-201) and *cf. Scleroderma*; moderate increase of *Sporormiella* (HdV-113), Sordaria (HdV-55A), *Cercophora* (HdV-112) and *Ceratophyllum* (HdV-137); continuous presence of *Chaetomium* (HdV-7A). *Mer-6a*: better representation of Apiaceae, Cichorioideae, *Nymphaea*, *Sparganium;* beginning of development of *cf. Debarya* and *Rivularia*-t. (HdV-170); last records of *Pseudoschizaea*; high concentrations of *Xylomyces* (HdV201), *Sporormiella* (HdV-113) and *cf. Scleroderma*. *Mer-6b*: increase in *Salix* and *Myriophyllum* (percentages and concentrations); decrease in Cichorioideae; high concentrations of *cf. Debarya* associated with HdV-128B, *Spirogyra*, *Aphanizomenon*, *Gloeotrichia* (HdV-146) and *Penium* (HdV-66 et HdV-333); decrease in *Xylomyces* (HdV201; maximum concentrations of *Ceratophyllum* (HdV-137); appearance of HdV-187B.
Mer-5	**Pollen** Very high herbaceous rates (~88%) with dominance of Poaceae (32-43%) and Cichorioideae (6-17%); increase of *Hordeum*-t. (2-5%), *Secale*-t. (0.7-4%), *Triticum*-t. (1-3%), *Plantago lanceolata*-t. (1-6%), *Polygonum aviculare*-t. (1-2%), Asteroideae (3-4%); Chenopodiaceae-t., *Artemisia*, *Rumex*, Brassicaceae, Fabaceae, Ranunculaceae also recorded (≤ 3%); decrease in Cyperaceae, *Sparganium*, *Typha latifolia*, *Nymphaea*, *Myriophyllum* and *Cannabis-Humulus*-t. *Alnus*, *Betula*, *Corylus* and *Quercus* are the best represented trees (≤ 6%); regular occurrences of *Salix*, *Fagus*, *Ulmus* and *Carpinus betulus*-t. **Algae** Maximum concentrations of *Gloeotrichia* (HdV-146) and *Pseudoschizaea*; presence of *Botryococcus*,

	Pediastrum, *cf. Aphanizomenon* and *Rivularia*-t. (HdV-170); sharp decline in concentrations of *Spirogyra* and *cf. Debarya*. **NPPs** Fall in concentrations (118-12,806gr/g); only *Sporormiella* (HdV-113) maintains its previous values; continued presence of *Sordaria* (HdV-55A) and *Glomus* (HdV-207); *Ceratophyllum* (HdV-137), Cladocerans and Chironomids stable; *Helicogermslita* (EMA-55), *Kretzschmaria deusta* (HdV-44), HdV-361, HdV-123, TM-4014 are no longer recorded.
Mer-4	**Pollen** Strong increase in pollen concentrations (15,547-131,094gr/g). The frequencies and concentrations of *Alnus* (6-30% and avg. 10,141gr/g) are increasing and to a lesser extent those of *Corylus* (2-5% and avg. 1,878gr/g), *Quercus* (4-7% and avg. 3,493gr/g) and *Fagus* (0.2-2% and avg. 453gr/g); *Carpinus betulus*, *Castanea* et *Ulmus* are noted more or less regularly. Herbaceous are extremely diverse (32-41 taxa) although their pourcentages are slightly decreasing (59-83%); high values of *Cannabis-Humulus*-t. (2-21% and avg. 4,696gr/g); development of helophyte and macrophyte herbaceous *Sparganium* (3-23%), *Typha latifolia* (0.4-5%), *Filipendula* (0-2%), *Potamogeton* (0-6%), *Nymphaea* (0-5%) and *Alisma* (<1%); Poaceae stable (16-30%); strong decrease of Cichorioideae (2-7%) and Cyperaceae (1-10%); slight increase (≤ 3%) of *Plantago lanceolata* and *Rumex*; regular records of *Centaurea cyanus*. **Algae** Development and diversification of algae; *Spirogyra* (ind., HdV-132 and HdV-342) is best represented and is accompanied by HdV-128, *cf. Debarya*, *Zygnema*, *Gloeotrichia* (HdV-146), *Rivularia*-t. (HdV-170) and HdV-229; occurrences of *Botryococcus*, *Mougeotia* and *Pseudoschizaea*. **NPPs** Maximum values in concentration (avg. 26179 gr/g) and in diversity (avg. 29). High increase of *Melanconis alni* (EMA-3), HdV-200, *Sordaria* (HdV-55A) et *Sporormiella* (HdV-113); more moderate increase of *Chaetomium* (HdV-7A), *Coniochaeta cf. ligniaria* (HdV-172), Coniochaetaceae-Xylariaceae, Sordariaceae, *Brachysporium* (HdV-359) ; decrease of scalariform perforations (HdV-114) ; appearance of *Ceratophyllum* (HdV-137), Cladocerans Chironomids et IBB-17 ; regular record of *Apiosordaria* (HdV-169), *Gelasinospora cf. retispora* (HdV-2), *Dictyosporium*, HdV-18, HdV-125, *Clasterosporium caricinum* (HdV-126), *Entyloma*-t., *Thecaphora* (HdV-364), *cf. Tilletia*, *Urocystis,* HdV-205 and Helminth eggs. *Mer-4a*: maximum values (percentages and concentrations) of *Alnus* and *Cannabis-Humulus*-t.; regular presence of *Ulmus* and *Vitis;* high values of *Melanconis alni* (EMA-3), *Sordaria* (HdV-55A), *Sporormiella* (HdV-113) and *Ceratophyllum* (HdV-137). *Mer-4b*: decrease in the mean arboreal pollen values (17-23%) induced by that of the percentages of *Alnus*; decrease in the diversity of arboreal taxa; increase in the frequencies of *Nymphaea* and *Myriophyllum*; decrease in the rates of *Cannabis-Humulus*-t.; maximum values of *Spirogyra*; appearance of *Botryococcus*, *cf. Debarya* and *cf. Aphanizomenon* ; *Zygnema* and *Gloeotrichia* (HdV-146) are no longer reported; maximum values of HdV-200; decrease of *Melanconis alni* (EMA-3) and scalariform perforations (HdV-114).
Mer-3	**Pollen** Minimum pollen concentrations (6,806-22,923gr/g). Strong increase in herbaceous taxa (74-80%) especially Cichorioideae (12-25%), Poaceae (14-35%) and Cyperaceae (11-24%); smaller increase (0.5-3%) in Apiaceae, Asteroideae, Brassicaceae, Ranunculaceae; presence of *Filipendula*, *Typha latifolia* and *Riccia*. Decrease of Alnus (10-16%); Corylus, Quercus stable; presence of *Fagus*, *Ulmus* and *Sambucus*. **Algae** Rare occurrences of *Spirogyra*. **NPPs** Increased concentrations of *Sordaria*-t. (HdV-55), *Cercophora*-t. (HdV-112), HdV-361 and scalariform perforations (HdV-114); presence of *Rhytidospora cf. tetraspora* (HdV-171) and HdV-200.
Mer-2	**Pollen** Increasing mean arboreal pollen values (39-65% and AP > NAP%) due to maximum values of *Alnus* (23-55%, 1,666-15,639gr/g); *Quercus* (4-7%) and *Corylus* (2-6%) stationary; regular presence (< 2%) of *Betula*, *Fagus*, *Ulmus*, *Tilia*. Herbaceous dominated by Poaceae (35-20% and 10,407-2,082gr/g) associated with Cichorioideae (2-4%) and Cyperaceae (2-5%); many other herbaceous recorded (< 3%) as Apiaceae, Asteroideae, *Plantago lanceolata*-t., *Hordeum*-t., *Triticum*-t., *Rumex*, Ranunculaceae, *Sparganium*. **Algae** Minimum concentrations (avg. 242gr/g); only *Spirogyra* is noted regularly; occurrences of HdV-128A, HdV-128B and *Rivularia*-t. (HdV-170). **NPPs** Appearance of *Melanconis alni* (EMA-3), increase in concentrations of scalariform perforations (HdV-114); *Chaetomium* (HdV-7A), Coniochaetaceae-Xylariaceae and TM-4014 stable; other previously reported taxa are decreasing or no longer recorded.
Mer-1	**Pollen** Non arboreal taxa (NAP) increasing from 62 to 84% dominated by Poaceae (28-49%, 4,295-25,401gr/g) associated with Apiaceae (0.9-15%), Cichorioideae (2-10%), Cyperaceae (3-14%), *Plantago lanceolata*-t. (2-3%) and *Rumex* (0.4-3%); many other herbaceous taxa recorded (≤ 3%) such as Brassicaceae, Fabaceae, Ranunculaceae, Rosaceae, *Sparganium*, *Callitriche*, *Potamogeon*, *Hordeum*-t. and *Triticum*-t. *Quercus* is the best represented tree taxon (5-22%, 645-19,014gr/g), accompanied by *Alnus* (3-10%), *Corylus* (1-4%), *Betula*

(0-1%), *Sambucus* (0.2-1%) and *Fagus* (0.4-2%).

Algae

Only *Spirogyra* is regularly recorded; irregular occurrences of *Zygnema*, *Rivularia*-t. (HdV-170) and *Pseudoschizaea*.

NPPs

Highest concentrations with continuous recording for Coniochaetaceae-Xylariaceae, *Sporormiella*-t. (HdV-113), *Sordaria*-t. (HdV-55), *Glomus* (HdV-207), *Chaetomium* (HdV-7A), *Cercophora*-t. (HdV-112) and HdV-361; irregular presence of *Helicogermslita* (EMA-55), *Kretzschmaria deusta* (HdV-44), TM-4014 and HdV-91; presence of scalariform perforations (HdV-114).

Mer-1a: maximum values of *Quercus* and Apiaceae; regular occurrences of *Castanea*.

Mer-1b: increase in Poaceae, Cyperaceae, Cichorioideae and *Equisetum*; decrease in *Quercus*, Apiaceae and *Rumex*; decrease in Coniochaetaceae-Xylariaceae, *Helicogermslita* (EMA-55), *Kretzschmaria deusta* (HdV-44) and TM-4014.

478

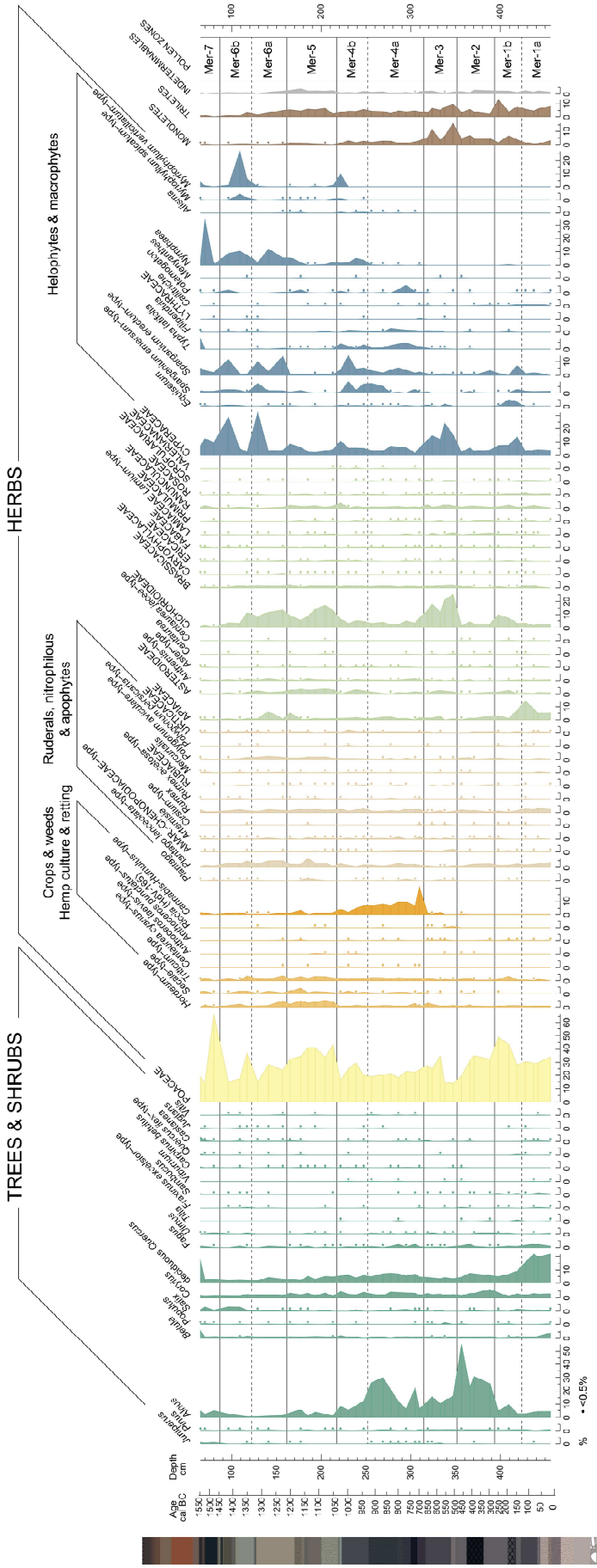

479 ***Fig. 8. Pollen percentage diagram with selected taxa from the Mérancis C0 core.***

480 ***Fig. 9. Concentrations of Algae, Fungi and other NPPs with selected taxa from the***

481 ***Mérancis C0 core. Curve exaggeration x10. The scale for concentrations values differs***

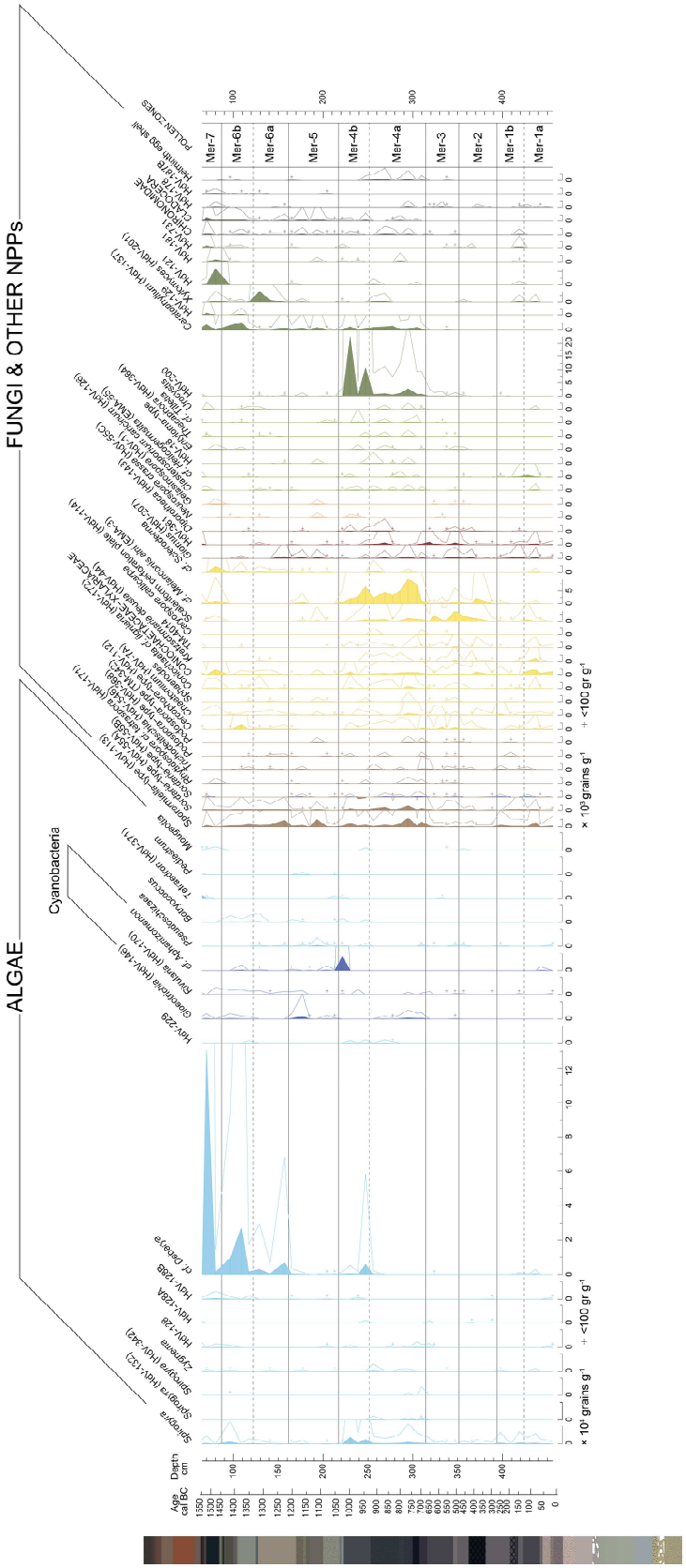

across algae and fungi & other NPPs.

4.2. The Ors mill reach

Nine cores, four trenches, and an electrical resistivity profile support our interpretation of the sedimentary architecture (Figs. 10 and 11). Resistivity values ranging between 99.7 and 154 Ωm correspond to the sands and gravels located in the western part of the profile. Values between 64 and 27.2 Ωm correspond to fine to the medium sands that made up the substrate or formed a large part of the sedimentation on the right bank of the Mérantaise river. The lowest values (≤ 17.7 Ωm) correspond to an organic-rich silty fill from one to three metres in depth mainly found on the left bank of the river. The results of sedimentological and geochemical analyses are shown in Figure 12. The proposed chronological division was derived from the age depth model proposed for the C5_MDO core and chronostratigraphic interpretations.

Fig. 10: Architecture and sedimentary filling at Ors mill.

A: Cross-sectional profile of electrical resistivity tomography, C0 and C2 coring, and ^{14}C dating; B: Description of the 10 sedimentary units. the description of units 5 7 and 9 is shown

499 *in* *figure* *11.*

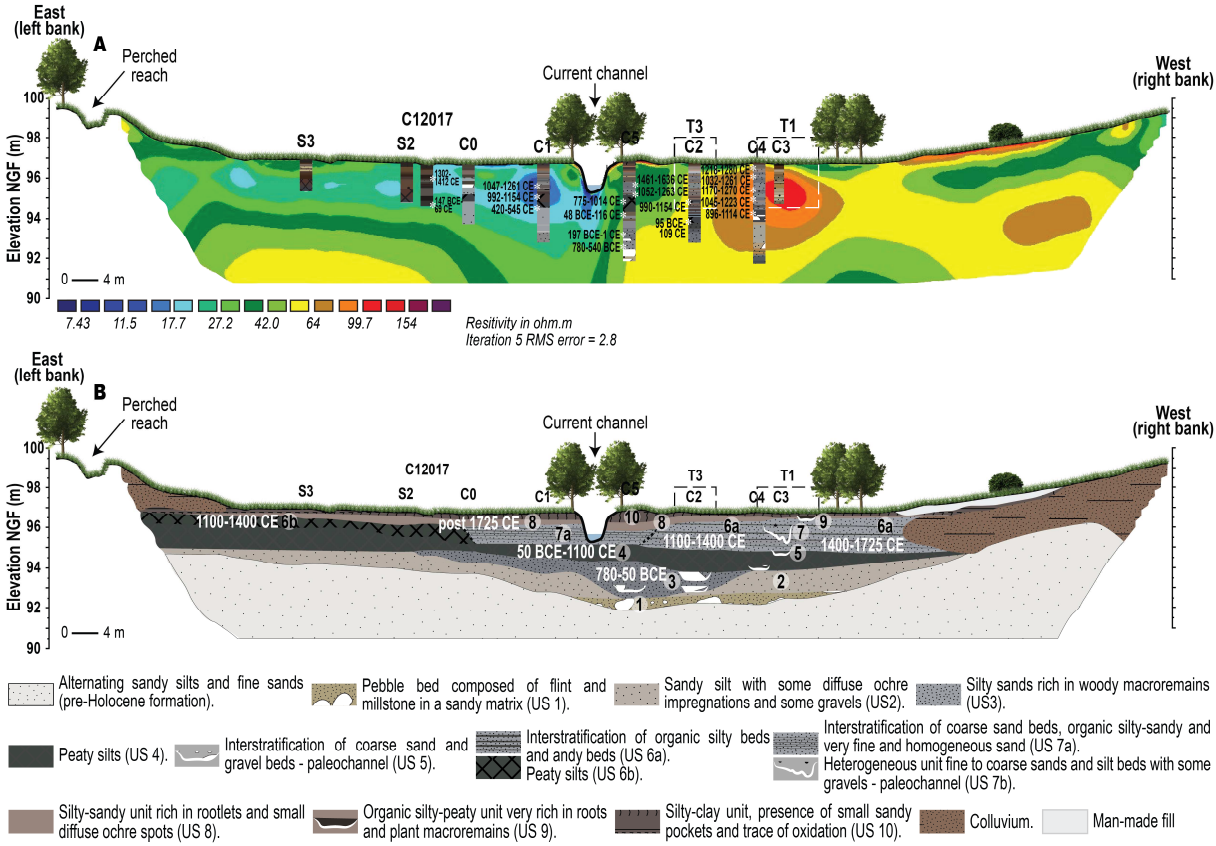

500

501

502 ***Fig. 11: Trench n°1.***

503 *The three dates in italics originate from trench no. 4.*

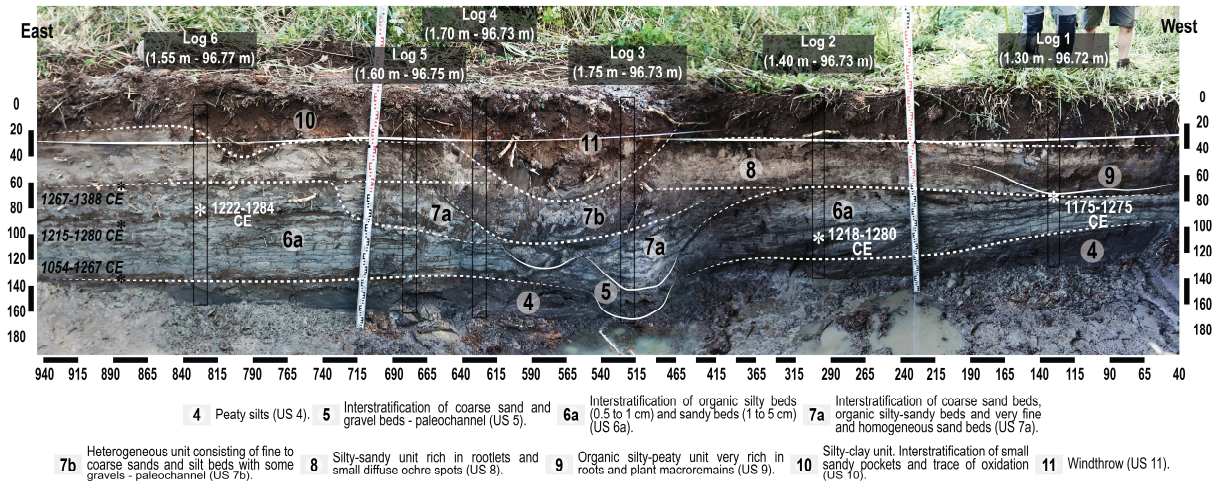

504

505

506 **Pre-Holocene formations**

Pre-Holocene formations were only observed in core C4 (Fig. 10). They comprised alternating dark gray sandy silts and fine ochre sands with ochre ferruginous concretions. These facies correspond to Fontainebleau sands most often reworked by pre-Holocene morphogenic processes.

Unit 1

This clastic unit, 27 cm thick in core C4, and 57 cm thick in core C5, was characterised by a multi-centimetric pebble bed, consisting of a mixture of flint and millstone pebbles embedded in an ochre sandy matrix. The MS showed a significant peak at the base, between 485 and 489 cm, around 220 and 1,132 x 10^{-5} SI. This unit corresponds to an undated channel bottom deposit.

Unit 2

This unit comprised a grey-beige sandy silt with a few diffuse ochre-coloured impregnations and some gravels. Very homogeneous and laterally extensive, it was identified in cores C0, C1 and C4. The base of the unit on C1 was sandier and may correspond to the proximity of the channel, while most of the sedimentation corresponded to overbank silts. It was not dated.

Unit 3 (*c.* 2730-2050 cal. BP; 780-50 BCE)

This unit, widely identified in the centre of the valley (C0, C1, C12017, C2, and C5), comprised primarily light grey silty sands rich in woody macroremains. In cores C2 (328.6-246.0 cm) and C5 (389.9-400 cm), the unit shows a coarser facies made of multi-centimetric pebbles in a silty matrix rich in woody macroremains. In cores C1, C12017, and C0, the sediments were less sandy, siltier, and more organic. In core C5, at the base of the unit,

between 440 and 372 cm, the MS was almost constant and low, characteristic of Fontainebleau sands poor in rutile and magnetic minerals. From 375 cm onwards, the Ti signal increased and remained generally homogeneous until the top of the unit. The MS increased with three peaks: 361-372 cm, 307-300 cm, 285-278 cm. This indicates poorly sorted sandy sediments with detrital arrivals resulting from the erosion of Lozère sands from the plateaus. The Fe/Ti ratio remained constant throughout the unit as did the concentration of Ca. Around 335-300 cm, a peak was observed in Ca but not in the Ca/Ti ratio, so the carbonate inputs were terrigenous and probably originated from Rupelian limestones. The Inc/Coh signal remained stable at around 3 cps but increased slightly at the top of the unit, while the sedimentation was silty and richer in organic matter. This unit can be interpreted as a riverbed with shallow, mobile channels in a silty-sandy alluvial plain.

Unit 4 (c. 2000-850 cal. BP; 50 BCE-1100 CE)

This unit was clearly distinguishable from previous units due to increased organic facies: dark brown to black peaty silts. It was more widely distributed on the left bank but was identified in all the cores and also at the base of trench no. 1 (Fig. 11). Some local variations were observed: in core C2, the unit was distinguished by blue-grey silty beds rich in macroremains, while in core C4, the base of this unit was a bed of centimetric gravels in a black, highly organic sandy-silt matrix. The MS was low (ranging from -0.9 to 2.8 x 10^{-5} SI). The Ti signal clearly decreased to 91-967 cps. The Fe/Ti ratio showed three significant increases: 260-245 cm, 230-222 cm, 190-20 cm, pointing to an increase in anoxic environments. The Ca signal was weak at the base and at the top. The Ca/Ti ratio showed three stages of authigenic carbonate inputs probably related to the rising water table (255-245 cm, 232-218 cm, 199-179 cm). The Inc/Coh signal remained constant and homogeneous (around 7 cps), consistent with the organic nature of the sedimentation. This unit, which

557 mainly reflected a palustrine environment with low detrital input, was dated with seven
558 radiocarbon dates, mainly to the 1st millennium AD (147 BCE - 1154 CE).
559
560 **Unit 5**
561 This unit corresponded to the filling of a small channel observed at the base of trench no. 1
562 (Fig. 11). This filling was characterised by interstratification of coarse sand beds and light
563 grey gravel beds incising the silty-peaty Unit 4.
564
565 **Unit 6 (c. 850-550 cal. BP; 1100-1400 CE)**
566 This unit was divided into two subunits. To the west, subunit 6a was characterised by
567 interstratification of brown organic silty beds (0.5 to 1 cm thick) and grey sandy beds (1 to 5
568 cm thick). This unit was found in cores C2, C4, C3, and was also clearly visible in trench n°1.
569 Thanks to six radiocarbon dates of the cores and six of trench n°1, it was dated between 1054-
570 1388 cal AD. The 1-1.5 m thickening of this sub-unit 6a, the horizontal arrangement of the
571 laminations and the absence of pedological features indicate deltaic-type sedimentation in a
572 submerged environment characterised by alternating flood deposits transporting material from
573 the slopes (Fontainebleau sands) and finer and organic sedimentation from receding flood and
574 standing water. This sedimentation testifies for the first time that a pond was established at
575 Ors mill and its use dated to the beginning of the 11th century. Subunit 6b was identified in
576 boreholes S1 and S2, and in cores C12017 and C0, and was located in the eastern part of the
577 alluvial plain. Dated to between 1154 and 1412 cal AD, it was sub-contemporaneous with
578 subunit 6a and showed that the organic peaty sedimentation that characterised unit 4
579 continued here. It reveals the existence of a dam forming a reservoir that occupies a large part
580 of the valley floor.
581

582 **Unit 7 (c. 550-250 cal. BP; 1400-1725 CE)**

583 This unit was identified in cores C0, C1 and C5 and in trench n°1. It comprised
584 interstratified coarse white-grey sand layers (1 to 5 cm thick), organic brown silty-sandy beds
585 (0.5 cm and 1 cm thick) and very fine and homogeneous grey sand beds. These facies, very
586 similar to those described in the previous unit, showed that it was the final stage of filling of
587 the pond, dated from the 15th to the 17th century with a radiocarbon date obtained from core
588 C5 (1461-1638 CE) and last recorded on the 1701 terrier plan (the only one to show a pond at
589 this location; CD78: archives_d1470). In core C5, the average grain size of the sandy laminae
590 was 295.2 µm. The MS increased slightly (from 1.7 to 6.7 x 10^{-5} SI). Measurements of major
591 elements revealed marked fluctuations depending on the type of bed. The sandy laminae had a
592 low concentration of Ti, and a low concentration of Fe. On the other hand, silty laminae
593 contained high concentrations of Ti and Fe. No variations were observed in the other major
594 elements with respect to the laminae. The Ca/Ti ratio was low, meaning most of the carbonate
595 inputs were terrigenous, except at the top of the unit.

596 In trench n°1, two sedimentary subunits with elevations and facies similar to unit 7 were
597 linked to it even though the sedimentation was not directly dated. Subunit 7a contained
598 interstratified coarse white-grey sand beds (1 to 5 cm thick), organic brown silty-sandy beds
599 (between 0.5 cm and 1 cm thick), and very fine and homogeneous grey sand beds. Subunit 7b
600 comprised heterogeneous sedimentation made up of fine to coarse grey sands and brown silt
601 beds with some gravels. These two units corresponded to the two successive fillings of a
602 channel, which was first filled by sediments characteristic of the pond fill then dredged out
603 and filled sediments, revealing the disconnection between the channel and the pond. We
604 hypothesise that the second stage corresponded to a drainage channel probably dug when the
605 pond was abandoned.

606

Unit 8 (post 1725 CE)

This unit was found over the entire alluvial plain and overlies the previous units. It corresponded to a homogeneous 40 cm thick layer of beige silty-sandy sedimentation rich in small diffuse ochre stains. In core C5, the MS increased from 6.7 to 14.5 x 10^{-5} SI throughout the unit. The concentration of Ti was high, and this unit had the highest Fe content, which can be explained by the abundance of iron concretions. It was the result of a complete silting of the valley bottom by overflow silt that subsequently underwent hydromorphic pedogenesis. This unit can be dated by looking at the map of the surroundings of Paris of the Abbé Delagrive dated 1731-1741 CE, which does not mention the existence of the pond, unlike all the later maps.

Unit 9

This unit was only identified in trench n°1. It comprised an organic brown silty-muddy sediment, very rich in root and plant macroremains that clogged a small channel about 20 cm deep, probably sub-contemporaneous with unit 8. This was interpreted as a small ditch dug to drain the meadows located in the valley bottom.

Units 10 and 11

Unit 10 was a brown silt rich in rootlets corresponding to contemporary soil developed under a damp meadow. Unit 11, identified in trench n°1, corresponded to a windfall.

Fig. 12: Sedimentological and geochemical analysis of core C5.

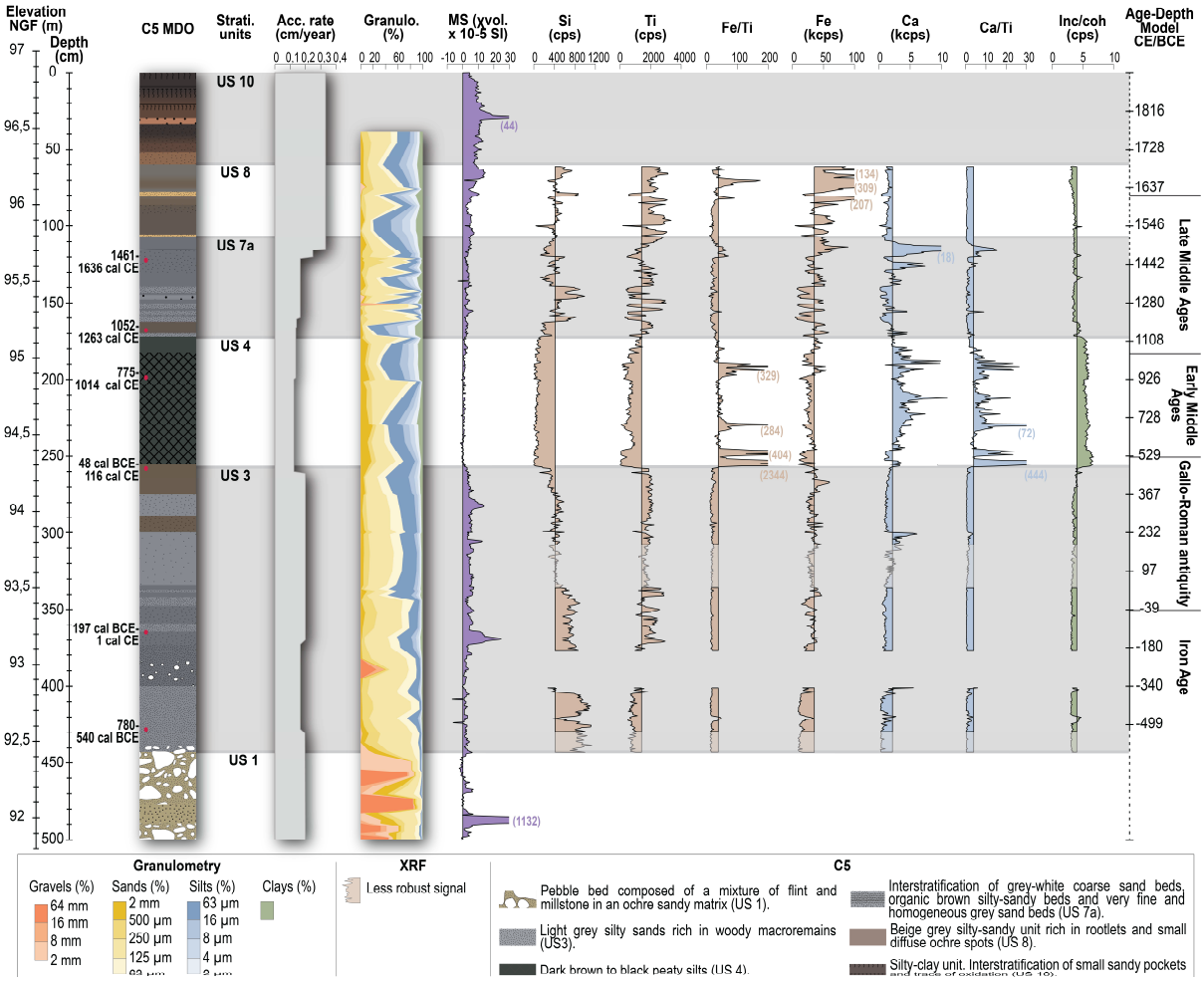

5. Discussion

5.1. The onset of Late Holocene sedimentation and the development of wetlands (before 500 CE)

5.1.1. A wandering channel in wetlands

Despite the expansion of farming on the surrounding plateaus from the Neolithic period on, like all the plateaus in the central Paris basin (Leroyer and Allenet, 2006), low sedimentation was observed prior to the Bronze Age. The middle Mérantaise valley has long been a transfer zone. At the base of the sedimentation, the alternation of channelized fluvial deposits, incising the substratum or the pre-Holocene formations, and silty-peat deposits were interpreted as the beginning of a Holocene alluvial aggradation. This remained moderate: 0.10 to 0.25 cm/year,

641 the product of fluvial flows in shallow channels (30 to 40 cm) filled with fine to medium
642 sands originating from the Fontainebleau sands, Lozère sands and silty formations from the
643 erosion of loess silts. Alluvial aggradation increased during the Gallo-Roman period (0.20 to
644 0.30 cm/year) (Fig. 7 and Fig. 12). The increase in silty inputs (terrigenous Ti and Ca)
645 indicates erosion of the soils of the plateaus and valley slopes, probably linked to increased
646 land clearing. Sedimentation during antiquity and the early medieval period indicates the
647 development of concentrated flows in the middle of a palustrine alluvial plain, without it
648 being possible to determine whether the fluvial style corresponds to a single wandering
649 channel or to anabranch flows.

650 The development of the palustrine spaces is supported by pollen record showing the
651 presence of helophytes and macrophytes taxa. The association of *Callitriche* and
652 *Potamogeton* is characteristic of vegetation growing in more or less running open water
653 (Bournerias et al., 2001; Fernez et al., 2015) together with *Spirogyra* and *Zygnema* algae. In
654 the waterlogged soils at the margin of the stream, sparse association of tall helophytes
655 reminiscent of reedbeds developed including *Sparganium emersum*-t., *S. erectum*-t.,
656 Apiaceae, Poaceae, Cyperaceae, *Equisetum* (Bournerias et al., 2001). The presence of this
657 assemblage was reinforced by the curve of *cf. Helicogermslita* (EMA-55), Xylariaceae
658 indicating Cyperaceae swamp environments (Prager et al., 2012). Finally, the association of
659 *Alnus*, *Populus*, *Fraxinus*, *Salix*, *Sambucus* and *Viburnum*, allows us to conclude on the
660 presence of a poorly developed riparian forest, in continuity with the reedbeds and wet
661 meadows. Beyond the wetlands, the low rate of Arboreal Pollen (AP) and its decrease from
662 (38% to 16%) point to an environment that progressively became more open at the beginning
663 of the pollen record (Mer-1, 10-275 cal CE) (Fig. 13). In the sub-zone Mer-1a, *Quercus*
664 values (~20%) and the diversity of tree taxa suggest the presence of remnants of a degraded
665 mesophytic forest similar to oak hornbeam or oak-beech forests. The local presence of

isolated groves is supported by the highest concentrations of the wood-parasitic fungus *Kretzschmaria deusta* (HdV-44) (van Geel and Andersen, 1988) and of Coniochaeataceae-Xylariaceae, most of which are associated with wood (Ellis and Ellis, 2017; Revelles et al., 2016). The dominant herbaceous taxa in Mer-1 are evidence for marshy areas surrounded by mesophilous and hygrophilous grasslands resulting from human activities: meadows used for hay mowing and/or livestock grazing. Ruderal, nitrophilous, and apophytes indicators (*Plantago lanceolata*-t., *Rumex*, Urticaceae, Amaranthaceae, *Artemisia* and *Polygonum aviculare*-t.) also confirmed the presence of livestock and trampled areas (Behre, 1981; Miras et al., 2015). Further evidence for the presence of livestock was also the relatively high concentrations of strict coprophilous and coprophilous/saprophytic fungi, such as *Sporormiella*-t. (HdV-113), *Sordaria*-t. (HdV-55A et HdV-55B), *Chaetomium* (HdV-7A) and *Cercophora*-t. (HdV-112). In this man-made environment, the continued presence (~2%) of *Hordeum*-t. and *Triticum*-t. points to the presence of cereal fields around the site (Hall, 1994). From 130 cal CE (Mer-1a / Mer-1b), declining values of *Quercus*, *Fagus* and *Kretzschmaria deusta* (HdV-44) indicate the reduction of the patchy degraded mesophitic woodlands. The significant increase in *Triticum*-t. (~3%) and Poaceae suggests that these clearings enabled the expansion of cultivated fields in the immediate vicinity of the site (Hall, 1994). In addition, a decline in the maintenance of the grassland vegetation by mowing and/or grazing is indicated by the decreasing values of coprophilous and coprophilous-saprophytic fungi and ruderal indicators, and appears to concern the wetter meadows, as indicated by an increase in Cyperaceae and Equisetum.

Between 275 and 485 CE (Mer-2), the high *Alnus* values (>25%) point to the local development of a dominant *Alnus* riparian forest (Huntley and Birks, 1983), accompanied in the understory by helophytes (Cyperaceae, Poaceae, *Sparganium*) and by numerous ferns. This interpretation is supported, on the one hand, by the appearance and expansion of *cf.*

691 *Melanconis alni* (EMA-3) - a fungus commonly found on dead alder twigs and branches
692 (Barthelmes et al., 2006) - and on the other hand, by scalariform perforations (HdV-114) often
693 correlated with bog alder groves (Pals et al., 1980; Barthelmes et al., 2006). Thus, it appears
694 that the abandonment of hay mowing and/or grazing of wet meadows recorded from 130 cal
695 CE continued until 485 cal CE. The presence of mesophilous grasslands is supported by the
696 dominance of Poaceae and the high herbaceous floristic diversity. Although some ruderal
697 indicators were present, the absence of coprophilous and coprophilous/saprophytic fungi
698 indicated the end of pastoral practices. In addition, the decrease in cereal values indicated a
699 shift from cultivated fields. Thus, this abandonment of the site recorded between 275 and 485
700 cal CE allowed the local development of an alder forest (Fig. 13).
701
702 *5.1.2. The specificities of the Mérantaise river in the northwest european context: the*
703 *maintenance of wetlands despite high anthropic pressure*
704 The limited pre-Bronze Age detritic sedimentation observed along the Mérantaise river is
705 consistent with the results of numerous studies conducted in the past two decades which
706 revealed clear evolutionary patterns in the valley bottoms of the northwestern european plains
707 and plateaus (Brown et al., 2018; Notebaert and Verstraeten, 2010; Verstraeten et al., 2017).
708 The expansion of highly organic sedimentation and low detrital sedimentation during much of
709 the Holocene has been attributed to the extensive forest development in the valley bottoms.
710 The forest covers limited runoff, and hence water erosion, as well as disturbing hydro-
711 sedimentary connectivity. In most small valleys in the central Paris Basin (Pastre et al., 2006),
712 organo-calcareous sedimentation was preserved at least until the Bronze Age. This
713 sedimentation is often very dilated, plurimetric, like in the valleys of the Beuvronne (Orth et
714 al., 2004) and Crould (Pastre, 2018) and, more broadly, in all valleys encased in a limestone
715 substratum in the Paris Basin (Lespez et al., 2008). The results obtained for the Mérantaise

river are in line with this general pattern but differ in the very low sedimentary aggradation until the Bronze Age in the two studied reaches. The sandy sedimentary formations in which the Mérantaise is incised, and the relatively steep slope of the valley bottom probably played a decisive role in favouring transfer rather than deposition of the sediments in the sections studied here.

From the Iron Age (800-52 BCE), the development of silty sedimentation can be explained by the retreat of the forest cover under the effect of cultivation of the watershed, as was the case in most north-west European river systems. The acceleration of detritic sedimentation was linked to the increase in cultivated land and in connectivity within catchments and marks the dominance of anthropogenic processes (Brown et al., 2018; Lespez et al., 2015; Verstraeten et al., 2017). This transformation very often had a threshold effect that caused a change in fluvial style, and in particular, the development of single channels within floodplains fed by constantly aggrading overflow silts (Broothaerts et al., 2014). While the phenomenon is ubiquitous in northwestern Europe, the timing of fluvial metamorphosis was specific to each watershed. Thus, comparing the Mérantaise with other rivers studied in the region provides a basis for discussion of the diversity of situations in the central Paris Basin, in an equivalent bioclimatic and anthropogenic context. In general, silty sedimentation occurred quite early, i.e., from the Bronze Age on. It is recorded in the Beuvronne valley (Orth et al., 2004) where it became dominant upstream in the Early Bronze Age (post 2000-1700 BCE) and subsequently became widespread downstream in the Iron Age (800-300 BCE). This happened later in the Crould valley (Pastre, 2018) where diffuse silty inputs dominated in the Iron Age (950-52 BCE), while organo-detrital sedimentation was generalised at the end of the Iron Age or during the Gallo-Roman period (350 BCE- 476 CE). The nature of the sandy substratum and the rise of the water table in the Iron Age, which characterised all the valley bottoms in the Paris Basin and more generally in northwestern

741 Europe (Magny, 2004), may have favoured hydro-sedimentary connections and the increased
742 efficiency of the sedimentary cascade from the cultivated plateaus in the small valleys of the
743 Paris Basin (Lespez et al., 2008; Pastre et al., 2002). Regional pollen records confirm the
744 observations made along the Mérantaise and show an increase grasses and anthropogenic
745 indicators evidence for a major increase in agriculture beginning in the Late Bronze Age
746 (David et al., 2012). During the Second Iron Age, the very significant development of La
747 Tène rural settlements (Blancquaert et al., 2002) and the reorganisation of rural life caused by
748 the Romans was responsible for the intensification of agriculture and the increase in
749 agricultural land.

750 After this first stage, the development of palustrine environments started towards the end
751 of the Gallo-Roman period, proof that, in this valley, detrital development did not reach an
752 irreversible threshold, as it did in many other valleys in and on its margins of the Paris Basin
753 (Lespez et al., 2015; Pastre et al., 2006). This observation confirms the wide variability of
754 silty sedimentation at regional scale but more generally in small and medium-sized
755 watersheds (Strahler order 2 to 5) as also observed in the Loire watershed in France (Morin et
756 al., 2011), in the Djile watershed in Belgium (Broothaerts et al., 2014) and in the Wetter
757 watershed in Germany (Houben et al., 2013). This observation can be explained by the
758 unequal efficiency of the lateral connectivity of different reaches along the same stream, the
759 differences in colluvial inputs from one reach to another, and/or to the unequal efficiency of
760 longitudinal connectivity. The abandonment of agropastoral activities in the valley bottom
761 during the late Roman Empire (275-476 CE) is reflected in regional pollen records, which
762 show a slight decline in anthropogenic indicators. This was accompanied by new peat
763 sedimentation, which does not necessarily indicate widespread human abandonment (Leroyer,
764 1997). Similar observations have been made in the Djile valley, confirming the decline of
765 agropastoral activities in the valley bottoms in many European regions from the end of the 3rd

766 century, some linked to the multiple instances of instability during the late Roman Empire
767 (Broothaerts et al., 2014).
768
769 ***5.2. Wetlands preserved despite intensified pressure on the valley bottom (c. 500-1050 CE)***
770 *5.2.1. The ecological impact of agropastoral activities on wetland margins (500-675 CE)*
771 At Mérancis, we observed the expansion of a palustrine environment marked by the spread
772 of authigenic organic and carbonate sedimentation, and also in the valley bottom at Ors mill,
773 where the presence of blue silt deposits indicated the presence of open water. Although on the
774 one hand, marshy environments persisted, on the other hand, paleo-biological data attest to
775 the extent of anthropogenic transformations following the previous abandonment. Between
776 485 and 675 CE, the decrease in *Alnus* values shows that riparian forest is cleared leading the
777 expansion of a tall helophytes vegetation with *Typha latifolia*, *Filipendula*, Cyperaceae,
778 Poaceae, *Sparganium erectum*, *Equisetum* and Pteridophytes. Pollen and NPP data reveal that
779 the clearing is the result of a second phase of agro-pastoral activities indicated by an increase
780 in trampling indicators (Chenopodiaceae, Brassicaceae, Poaceae, Cichorioideae, Asteroideae,
781 *Plantago*) (Behre, 1981; Bournerias et al, 2001), grazing on wet meadows (high Cyperaceae
782 combined with decreasing *Alnus* values) (Lagerås et al., 1995) and on dry meadows (regular
783 presence of *Juniperus* and Ericaceae) (Behre, 1981; Berglund et al., 1986; Gaillard et al.,
784 1991; Bournerias et al., 2001; Rasmussen, 2005). The local presence of grazing herbivores is
785 also supported by an increase in dung-related fungi (*Rhytidospora cf. tetraspora* (HdV-171),
786 *Sordaria*-t. (HdV-55A), *Sporormiella*-t. (HdV-113), *Trichodelitschia* (HdV-546),
787 *Cercophora*-t. (HdV-112), *Chaetomium* (HdV-7A), *Sphaerodes* (TM-020)). The concomitant
788 presence of fire-promoted fungi (*Neurospora crassa* (HdV-55C) and *Gelasinospa* (HdV-1))
789 suggests the possible use of fires (Innes and Blackford, 2003; van Geel and Aptroop, 2006;
790 Cugny, 2011) by burning felled tree for clearing (Behre, 1988). The extension of open

outfields areas and agro-pastoral activities caused increasing soil erosion as shown by the increase in concentrations of *Diporotheca* (HdV-143), *Glomus* (HdV-207) and HdV-361 (Hillbrand et al., 2012; Revelles and van Geel, 2016; Enevold et al., 2019). The moderate increase in *Hordeum*-t. and *Triticum*-t. values associated with the presence of *Anthoceros laevis*-t., *Anthoceros punctatus*-t. and *Riccia* support local cultivated fields near the site (van Geel, 1986). From 580 CE onwards, in addition to cereal cultivation, the hemp cultivation is attested by a continuous curve (<5%) (Whittington and Edwards, 1989; Lavrieux et al., 2013; Reinbold, 2017).

5.2.2. Aquatic environment and the development of agricultural activities (675-1035 CE)

Thereafter, and until the year 1,000, major shifts appeared in the pollen record, coinciding with the transition to organic brown clayey silts and an increase in the rate of sedimentation at both study sites. At Mérancis, pollen data indicate the expansion of helophytes and macrophytes taxa together with the increase and diversification of algal flora (HdV-128, *cf. Debarya*, *Spirogyra*, *Zygnema*, HdV-229) (Supplementary S5). The increase in this aquatic vegetation indicated the presence of a meso-eutrophic, moderately deep and weakly running fresh water body (Fernez et al., 2015), favouring the presence of Chironomids and Cladocerans, whose regular occurrences were recorded from 675 CE on. The establishment of a permanent water body coincided with a marked increase in the cultivation of hemp. The diversification and the marked increase in the concentrations of spores of strict coprophilous fungi (*Sporormiella*-t. (HdV-112), *Sordaria*-t. (HdV-55A), *Podospora*-t. (HdV-368 and TM-342), *Rhytidospora cf. tetraspora* (HdV-171), *Trichodelitschia* (HdV-546)) illustrate high livestock use, probably related to the watering place that can be used as drinking trough.

5.2.3. Hemp retting: paleobiological and sedimentological signatures

816 The sharp increase in *Cannabis-Humulus-t.* (21.2% and 4,696 gr/g on average) from 675
817 CE onwards probably indicates hemp retting in water (see below). The threshold for pollen
818 percentages of *Cannabis-Humulus*-t. used to determine hemp retting differs among authors,
819 thus making it difficult to compare: 8-10% (Whittinghton and Edwards, 1989; Lagerås, 1996),
820 20-30% (Peglar et al., 1989; Latałowa, 1992; Mercuri et al., 2002; Laine et al., 2010;
821 Lavrieux et al., 2013; Larsson and Lagerås, 2015) or above 40% (Bradshaw et al., 1981;
822 Gaillard et al.,1991; Schofield and Waller, 2005). However, at Mérancis, the expansion of
823 *Cannabis-Humulus-t.* was concomitant with records of cyanobacteria *Gloeotrichia* (HdV-146)
824 and *Rivularia* (HdV-170) and then of *cf. Aphanizomenon*, indicating eutrophication of the
825 waters possibly due to retting (van Geel et al., 1994; van Geel et al., 1996) and is considered
826 by Reinbold (2017) to be one of the most reliable indicators. In parallel, macrophytes taxa
827 develop in the following succession *Ceratophyllum* (HdV-137), *Potamogeton*, *Nymphaea*,
828 *Myriophyllum spicatum*-t. and *Myriophyllum verticillatum*-t. Many studies (Bradshaw et al.
829 1981, 2005; Riera et al. 2006; Schofield and Waller 2005; Rasmussen 2005; Laine et al. 2010)
830 link the macrophytes rise to increasing nutrient concentrations caused by retting. Along with
831 the increase in *Cannabis-Humulus*-t., a sharp increase in HdV-200 fungi was also observed.
832 This fungal spore proliferates after an aquatic phase on drying stubble and dead plant remains
833 (van Geel et al., 1989; Kuhry, 1997). The correlation between the simultaneous maxima in
834 *Cannabis-Humulus*-t. and HdV-200 supports the hypothesis that retting begins in stagnant
835 water, followed by a drying phase to activate fungal decomposition of organic matter.
836 Further, high MS values and a peak in Mn, disconnected from the Fe signal, were
837 observed, indicating the development of non-terrigenous magnetism. Water retting allows
838 anaerobic pectinolytic bacteria to develop on the stems. *Bacillus* sp. populations dominated
839 during the first 40 hours of water-retting process, but as the water tanks begin to lack oxygen,
840 Clostridium sp. populations take over and become dominant (Mazian, 2018). Yet Bacillus

841 spores are paramagnetic due to the high concentrations of manganese accumulated in nucleus
842 and wall (Xu Zhou et al., 2018). Thus, the concomitance of MS, carbonate, and manganese
843 peaks could be considered as a sedimentological indicator of water-retting in the valley
844 bottom at Mérancis (Fig. 7).

845 At the same time, low values of *Alnus* (<10%) decline in scalariform perforation (HdV-
846 114) and high increase of *cf. Melanconis alni* (EMA3) were recorded. This pathogenic
847 fungus, which is associated with cankers and branch dieback in *Alnus* is linked to over 90%
848 mortality in alder (Sieber et al. 1991). By causing significant degradation of water quality,
849 retting can harm the riparian flora (Sapin and Virassamy, 2020) which allows us to
850 hypothesise dieback of the degraded wet alder forest following an infection by *cf. Melanconis*
851 *alni* (EMA-3). The maxima values of *Cannabis-Humulus*-t. were associated with the first
852 records of *Centaurea cyanus*-t., *Convolvulus*, *Polygonum persicaria*-t. and with an increase in
853 *Rumex*, and *Polygonum aviculare*-t values. These common weeds in cultivated fields can be
854 linked with hemp cultures and has been interpreted as possible indicators for crops rotation of
855 hemp with winter cereals (Whittington and Edwards, 1989; Gaillard et al., 1991; Latałowa,
856 1992). From 675 to 1035 CE, the creation of a water body for retting (pit or basin) in a
857 landscape composed of hay meadows, pastures, and cultivated fields is corroborated at
858 Mérancis. The absence of an identical MS signal at Ors mill, where the Ca signal was
859 confirmed, shows that retting was not practised throughout the valley bottom, but was
860 confined to certain locations, even though its importance has been confirmed at regional scale
861 by historical sources (Berthier, 2007; Schroeder, 2019). Retting was practiced in pits dug
862 along the river channel to take advantage of flowing rather than stagnant water, as shown by
863 numerous studies conducted in the Paris region (Berthier, 2007). The wooden pile found in
864 Core C0_Merancis could be one of the elements supporting the banks.
865

5.2.4. The decline of farming in the High Middle Ages and specialisation in the valley bottoms

During the High Middle Ages, a decrease in detritic sedimentation and an increase in organic sedimentation were widely observed in the Paris Basin, as in most of northwestern Europe. This was accompanied by reafforestation of valley bottoms and slopes. This reforestation explains the decrease in connectivity between plateaus, slopes and valley bottoms, which in turn limited the supply of sediments to the alluvial plains. The same observations were made both on the Seulles valley in Normandy (Beauchamp et al., 2017a), and in the central Paris basin, for example, in the Beuvronne and Crould valleys (Orth et al., 2004; Pastre et al., 2002) and more generally in Belgium (Broothaerts et al., 2021), Germany (Houben et al., 2013) and the Netherlands (de Moor et al., 2008). These observations correspond to a decline in the cereal cultivation, and were partially replaced by pastoral activities. This decline took place in parallel with the emergence of specialized activities such as hemp retting or the use of hygrophilous meadows for pastoral activities. In northwestern Europe, the peak of hemp cultivation occurred at similar or slightly later dates than those recorded on the Mérantaise. For example, in the midlands in England, the peak occurred between 340 and 895 CE while in the south-east of England it occurred around 1020-1210 CE (Schroeder, 2019), and in the Netherlands, around 900-1500 CE (Schroeder, 2019). Hemp cultivation was often combined with the use of the valley floor for pastoral activities, which can also be hypothesised for the Ors mill reach.

5.3. Hydraulic works and their impact on the valley bottom (after 1050 CE)

5.3.1. Artificial ponds and eutrophication (1050-1725 CE)

In the 11th century CE, a very clear change in sedimentation appeared at both studied sites, where sedimentation, typical of reservoir filling, was observed. At Ors mill, the regular sedimentation was characterised by laminations formed by sands brought by the floods and

891 silty deposits caused by decantation. From the 15th century onwards, the identification of
892 channels marked by the collapse of the banks and the imbrication of filling sequences suggest
893 a partial and seasonal drying out of the pond and a seasonal reduction in its dimensions and
894 partial cleaning operations. At Mérancis, the silty deposit indicates sedimentation associated
895 with a calm flow (Unit 5; Fig. 6). Between 1200 and 1450 CE, the more detritic sub-unit 5b
896 (Fig. 6) marked the beginning of pond filling, while the more organic sub-unit 5c marked the
897 gradual abandonment of the pond (Fig. 6). Since Ors mill is located downstream of the
898 Mérancis mill, the internal sedimentary structure of the pond filling must be considered an
899 explanation of this difference rather than trapping of coarse particles behind the upstream dam
900 (Mérancis). In fact, the core samples taken from Ors mill were located more than 75 m
901 upstream of the old dam, whereas those from Mérancis were located less than 25 m from the
902 dam. In the first case, at Ors mill, sedimentation was characteristic of the supply by the main
903 channel of the pond and corresponded to a subaquatic deltaic type of sedimentation. In the
904 second case, at Mérancis, the greater distance from the river sources prevented the coarsest
905 fraction of the sediments from entering the record. The low Ti content of the sandy facies
906 indicates that the sandy sediments were mainly Fontainebleau sands originating from the
907 channels incised in these formations or from gullying on the lower slopes. The silty facies,
908 rich in Ti and with a grain size close to that of the plateau silts, point to erosion of the topsoil
909 horizons of the plateaus. The increase in carbonate terrigenous inputs observed at Ors mill
910 reinforces the hypothesis of an increase in runoff on the slopes and the beginning of channel
911 incision in the substrate formations (Étampe limestone).
912 Sedimentary filling from 0.18 to 1 m thick was observed in the Ors mill pond (about 1 ha)
913 and about 1 m thick at Mérancis (about 3.1 ha). At both sites, the accumulation rates did not
914 increase significantly over those in the previous period (0.4 cm/year) and the aggradation
915 trend continued. The siltation of the Mérantaise ponds and forced sedimentation have slightly

accelerated sediment storage, but the construction of the dams did not significantly affect the rate of sedimentation in the valley bottom. On the other hand, the trapping of a sandy sedimentation over two thirds of the width of the valley bottom did profoundly alter the previous sedimentary model and revealed the weight of hydraulic developments by trapping sand sedimentation.

Pollen and NPPs analyses enabled a good understanding of the ecological consequences of constructing the dam and the pond by demonstrating ecological transformations in three successive phases as long as all ponds operated. From c. 1035 CE onwards, a decline in the riparian forest, and in particular of the alder groves, was recorded, which appears to be definitive (*Alnus* ~3%), as well as the end of fungal spore records related to afforestation, and more specifically to *Alnus* (e.g., *Kretzschmaria deusta* (HdV-44), Coniochaetaceae-Xylariaceae, *cf. Melanconis alni* (EMA-3) and scalariform perforations (HdV-114)). At the same time, macrophytes and helophytes, although still recorded, declined sharply, testifying to shrinkage of the wetlands at Merancis. The stable concentrations of *Ceratophyllum* (HdV-137), Chironomids and Cladocerans and algae are evidence for the establishment of ponds. The drop of *Cannabis-Humulus*-t. frequencies (~1%), concomitant with the disappearance of HdV-200, showed when retting ceased at this site. Cereal farming was increasing, as demonstrated by the increase in *Hordeum*-t., *Secale*-t., and *Triticum*-t., which cumulatively ranged from 6% to 12%, at the limit of values recorded in cultivated fields (Hall, 1994). The high proportion of Poaceae (32-43%) confirmed the local presence of cereal fields (Vuorela, 1973). These species were associated with an increase in ruderal and apophytes indicators (*Plantago lanceolata*-t., *Polygonum aviculare*-t., *Rumex*, Chenopodiaceae-t.), regular records of *Centaurea cyanus*-t., *Polygonum persicaria*-t., *Mercurialis* and *Artemisia* and the presence of *Anthoceros laevis*-t., *Anthoceros punctatus*-t. and *Riccia*. The development of cultivated fields led to a reduction in grazing land, demonstrated by the decrease in the concentrations of

spores of coprophilous fungi. The algal flora was dominated by the cyanobacteria *Gloeotrichia* (HdV-146), *cf. Aphanizomenon* and *Rivularia* (HdV-170), and a marked decrease in *cf. Debarya*, *Spirogyra*, *Zygnema* showing that the degree of eutrophication of the waters was still high.

An increase in algal concentrations was observed between 1215 and 1445 cal CE, mainlydue to *cf. Debarya*. The diversification and expansion of algae was accompanied by the notable development of the macrophyte herbaceous Nymphaea, *Potamogeton*, *Myriophyllum spicatum*-t., *Myriophyllum verticillatum*-t., *Ceratophyllum* (HdV-137) and of the helophyte herbaceous *Sparganium erectum*-t. and *Sparganium emersum*-t. associated with Cyperaceae. The expansion of algal and submersed aquatic flora, characteristic of vegetation growing in still open water, indicated a pond-like water body (van Geel et al., 1989; Bournerias et al., 2001; Carrión, 2002; John et al., 2002; Fernez et al., 2015; Guiry and Guiry, 2022) bordered by reed bed-type vegetation (Fernez et al., 2015). The sharp increase of *Xylomyces* (HdV-201), a saprophytic fungus growing on helophytic plants (van Geel et al., 1989; Kuhry, 1997; Cugny, 2011), as well as that of Chironomids, Cladocerans and other invertebrates (HdV-178, HdV-187B), confirm the presence of a pond containing rather stagnant water that may be subject to temporary dry periods (van Geel et al., 1989; Cugny, 2011). Their presence also suggests that mills associated with ponds are operated by releases with seasonal low flows in late summer and early autumn. The high values of *Hordeum*-t., *Secale*-t., *Triticum*-t., Poaceae, and apophytes and ruderal indicators (*Plantago lanceolata*-t., *Rumex*, *Polygonum aviculare*-t.) show that locally cultivated fields were still extensive at that time. From 1330 CE around, the slight increase in *Salix* frequencies is a signal that pioneer thickets were beginning to colonise the reedbed vegetation (Fernez et al., 2015), which may have been the result of less intensive use of the water infrastructure, while the decline in cereal pollen and ruderal indicators suggests a reduction in arable agriculture. It is worth noting that the period between 1330 and

966 1445 CE corresponds to a major demographic crisis throughout Europe, when that the
967 population of the Parisian agglomeration decreased from 250 to 100-150k inhabitants (Bourlet
968 and Layec, 2013) due to Black Death as well as the Hundred Years War.

969 From c. 1445 to 1550 CE, the permanence of the pond is marked by an increase in algal
970 and invertebrate concentrations. Algal flora was dominated by cf. Debarya, associated with
971 Tetraedron, Pediastrum, Mougeotia, Spirogyra and Zygnema. This planktonic association,
972 which is common in ponds, is associated with aquatic macrophytes (John et al., 2002). The
973 development of *Nymphaea* (pollen and HdV-129) to which can be added the high
974 concentrations of HdV-121, HdV-181 and HdV-731, NPPs related to meso-eutrophic
975 freshwater environments and helophyte vegetation (Pals et al., 1980; van Geel et al.
976 1982/1983; Bakker and van Smeerdijk 1982), suggest fluctuating water levels (Kuhry 1997;
977 van Smeerdijk 1989). Furthermore, the decrease in site frequentation was demonstrated by the
978 development of a ruderal elm/oak forest group developing from formerly pastured and farmed
979 lands (Bournerias et al., 2001), the decrease in cereal pollen and anthropogenic indicators, as
980 well as the almost complete absence of coprophilous fungi. While the reservoir, and
981 presumably the associated mills, continued to function the valley bottom appeared to be
982 marked by a decline that heralded reorganisation of valley bottom landscapes that extended
983 into the early 18th century.

984

985 *5.3.2. Hydraulic reorganisation and abandonment (1725-2020 CE)*

986 At the beginning of the 18th century, the Ors mill pond was abandoned, while the Mérancis
987 pond continued to be used until the 19th century, but then contracted considerably. At Ors
988 mill, the silt deposited by the flooding of the Mérantaise may have been favoured by a new
989 development of the valley bottom, indicated by drainage and/or irrigation ditches (units 9 and
990 10; Fig. 10 and Fig. 11). In the medieval and modern periods, the water meadows were

991 irrigated in the cold season to supply the nitrogenous elements essential for grass growth as
992 well as to thermally regulate the hay meadows to promote their productivity and improve the
993 quality of the hay (Benoit et al., 2003). At the same time, milling was being reorganised.
994 Indeed, the end of the pond did not imply abandonment of the mill, but corresponded to the
995 introduction of a bypass system based on the creation of an artificial reach that fed the mill
996 located at the end of the old causeway. This system functioned until 1866. The channel that
997 exists today was established at that time and its oversized geometry testifies to recurrent
998 cleaning (Jugie et al., 2018). This re-dredging coincided with the highest sedimentation rate
999 recorded in the reach. At Mérancis, the pond started to disappear in 1802 and the mill was
1000 subsequently abandoned. The sluice gates were opened and only the dike remained, which
1001 became which no longer hindered the passage of the sediments, hence the slight decrease in
1002 the sedimentation rate compared to the previous period. The former pond was transformed
1003 into a marsh formed by a hydraulic wasteland dominated by alder trees.
1004
1005 *5.3.3. The impact of hydraulic engineering on ecological and hydro-sedimentary dynamics*
1006 The 2nd millennium CE in Europe was characterised by the scale of hydraulic
1007 developments (Brown et al., 2018; Lewin, 2010). Research conducted in the Mérantaise
1008 Valley shows that pressure was very strong in the proximity of large cities due to the demand
1009 for food and the need for significant investments. In the Paris region, even if the development
1010 of mills began in antique times and continued during the Carolingian period, the pressure
1011 really only became strong in the 11th and 12th centuries. At the end of this period, the rivers
1012 were fully equipped (Benoit et al., 2003; Rouillard et al., 2011). At the time, the Mérantaise
1013 river had at least the eight mills that still functioned in the 18th century, and geoarchaeological
1014 studies confirm similar pressure in the Paris region, for example on the Crould river
1015 (Bensaadoune et al., 2005; Pastre, 2018). To the pressure caused by the construction of

hydraulic infrastructure, was added that of the potentially irrigable grasslands that they could contain. Indeed, in the few decades leading up to 1150, in response to growing demographic pressure, valley bottoms were acquired by aristocrats and monastic orders (Benoit et al., 2003). This led to an increase in productive activities with notable hydrological and ecological consequences. The emergence of cultivated fields and hay meadows favoured the development of ruderal plants and weeds, but restricted the riparian zone as early as the High Middle Ages, as observed in many European regions (Broothearts et al., 2014; Brown et al., 2018). On the Mérantaise river, anthropic pressure did not lead to the disappearance of wetlands since they were maintained before being artificially favoured by the construction of reservoir from the 11th century on. Indeed, our study shows that at Mérancis, the ponds were surrounded by hydrophilic vegetation while at Ors mill, marsh vegetation continued to grow at the margins of the pond. However, the wetlands and aquatic environments were gradually degraded. Milling reduced the oxygenation of rivers and increased sedimentation of poorly decomposing organic matter. At the same time, the development of crops and especially of livestock in the valley bottoms led to an increase in the nutrient load of small water bodies (Grönlund et al., 1986). In addition, it is likely that these ponds were also used for fish farming, as was the case of most the medieval ponds in northern France (Benoit et al., 2003; Rouillard et al., 2011). These activities stimulated eutrophication and favoured the development of cyanobacteria recorded in the Mérantaise basin between the 11th and 14th centuries. In many cases, these cyanobacteria radically modified the wetland and aquatic ecosystems of the medieval period (e.g., Bradshaw et al., 2005), which explains why in the Paris region, as early as 1678, retting was forbidden due to significant pollution of the rivers, and in particular eutrophication, and the presence of nauseating odours (Berthier, 2007).

From a hydro-sedimentary point of view, the establishment of dams and mills was accompanied by an increase in silty sedimentation in the valley bottoms of northwestern

1041 Europe during the Middle Ages (Brown, 2009; Brown et al., 2018; Notebaert and Verstraeten,
1042 2010). This phenomenon can be explained by the crossing of a threshold in the efficiency of
1043 hydro-sedimentary connectivity rather than by the increase in cultivated land subject to soil
1044 erosion (Houben et al., 2013; Verstraeten et al., 2017). In small streams, the highest
1045 sedimentation rates frequently coincided with maximum density of mills, which was the case
1046 on the Mérantaise and Normandy streams (Beauchamp et al., 2017a; Lespez et al., 2015).
1047 Unfortunately, sedimentary fills of ponds fed by small river systems are still too rarely studied
1048 to ensure reliable assessment. Such investigations, which are mostly performed in the United
1049 States, have been based on topographic approaches and channel geometry. For example, dams
1050 constructed on certain rivers in the mid-Atlantic region in the colonial era are known to have
1051 accelerated sedimentation in valley bottoms, resulting in a rise in alluvial plains of between 2
1052 and 5 m (Merritts et al., 2011; Walter and Merritts, 2008). However, other authors (Donovan
1053 et al., 2016) pointed out that the role of dams is more difficult to establish, as the aggradation
1054 of alluvial plains is ubiquitous and is not necessarily linked to former reservoirs. Observations
1055 made on the Mérantaise River are in line with the second line of thought: alluvial plain
1056 aggradation continued at a slightly higher rate but with no break between earlier and later
1057 aggradation rates, and with alluvial plains remaining entirely submerged during annual floods
1058 (Jugie et al., 2018).

1059 Most mills on small streams in northwestern Europe were built on courses set up as
1060 diversions from a weir to a reach (leat) that required most of the flow to turn the mill wheel at
1061 the expense of the existing channel (Lespez et al., 2015; Brown et al. 2018). The few
1062 available studies show that the increase in sedimentation occurred at the same time as these
1063 systems were established (Beauchamp et al., 2017a; Maaß and Schüttrumpf, 2019), as
1064 observed in the later period of Ors mill. This is because the weirs increase the level of the
1065 upstream water tables, thereby facilitating overflow and flooding of the alluvial plain during

floods (Maaß and Schüttrumpf, 2019). This increase in overflow frequency helps explain the aggradation of medieval alluvial plains under the influx of overflow silt, especially since this operation was considered by medieval and modern societies to enrich valley bottom meadows with nutrients (Benoit et al., 2003). However, after a certain period of time, the raising of the banks reduced the frequency of overflow plus, conversely, increased incisions and erosion of the banks, due to the increase in shear forces accentuated by dredging - as observed on the Geul in Germany (Maaß and Schüttrumpf, 2019) and on the Seulles in Normandy, France, (Beauchamp et al., 2017a). The late implementation of the bypass system at Ors mill explains why these consequences were not fully realized on this reach of the Mérantaise and why overflow capacities persist despite the strong alteration of channel geometry (Jugie et al., 2018).

Fig. 13: Evolution of the floodplain and hydraulic pressure on the Mérantaise over the last 3,000 years. Sources used: Bourlet and Layek, 2013; Marchandin, 2021

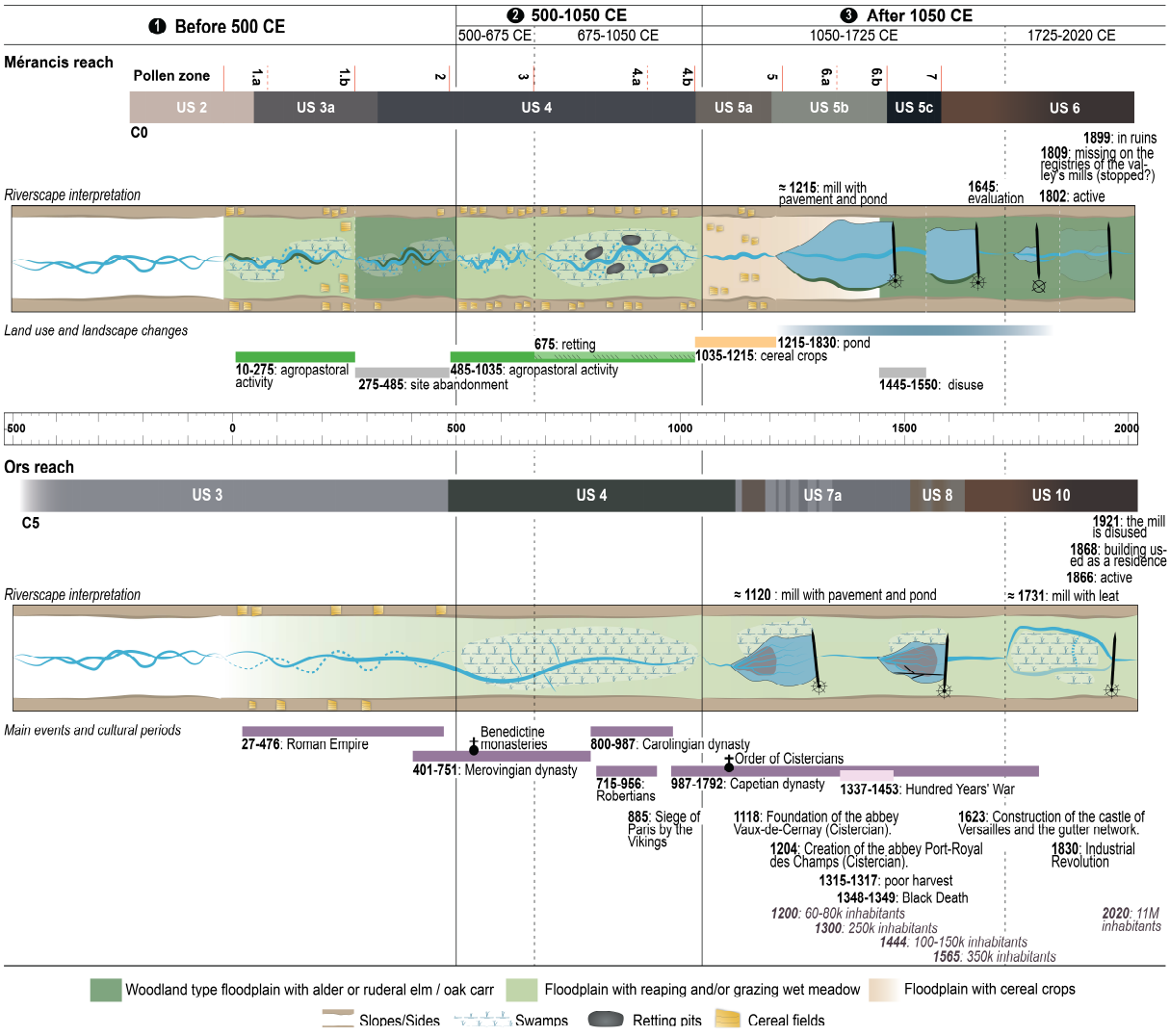

6. Conclusion

This article contributes to ongoing reflection on the hydro-sedimentary and ecological consequences of the transformation of a small watershed through agropastoral practices and the building of hydraulic structures during the recent Holocene. Reconstruction of the hydro-sedimentary evolution of the Mérantaise valley shows a general trend that matches that observed in Western Europe with an acceleration in sedimentary aggradation in the last three thousand years. The first aggradation lasted from the end of the Bronze Age to the beginning of the Iron Age and is probably explained by the retreat of the forest cover linked to cultivation of the watershed. During the Gallo-Roman period, aggradation continued but the

development of marshy environments shows that if soil erosion rate increased it did not reach an irreversible threshold, in contrast to what can be observed in many small valleys in northwestern Europe. Thus, wetlands continued to occupy a large part of the valley floor during the Middle Ages. Inherited from the previous periods or artificial (mill ponds), they are under pressure from human activities linked to both the investment capacity and needs of Paris.

From the High Middle Ages (7th c. CE), hemp retting was added to agropastoral activities and cereal cultivation, and for the first time, here we present sedimentary indicators of this activity in addition to the evidence provided by pollen records. The research also demonstrates the consequences of the hydrological engineering on the ecological functioning. Beyond the sedimentary aggradation and the transformation of the vegetation, it underlines the ecological consequences for the remaining and the artificial wetlands. The impact of retting and the agro-pastoral development is at the origin of mostly organic pollution accompanied by eutrophication of the aquatic environments. This attests to the transformation of wetland vegetation, riverine vegetation, and water quality over the last 1,500 years and is linked to the intensified use of small rivers in northwestern Europe, which was very clear in the study area because of the early emergence of urban demand and the increasing need to supply the city with energy, plant and food resources, long before small rivers were directly affected by urbanisation.

Sample credit author statement

Lucile de Milleville: Field Investigations, Sedimentary analyses. Writing – Original Draft. **Laurent Lespez:** Supervision, Field Investigations, Writing - Review & Editing. **Agnès Gauthier:** Pollen and NPPs analyses, Writing – Original Draft. **Frédéric Gob:** Field Investigations, Review & Editing. **Clément Virmoux:** Geophysical investigation, Writing -

Review & Editing**. Ségolène Saulnier-Copard:** Sedimentary analyses. **Valentine Fichet:** Pollen and NPPs analyses preparation. **Manon Letourneur:** Field Investigations. **Marion Jugie:** Historical and Field investigations. **Marta Garcia:** XRF core scanner analyses. **Kazuyo Tachikawa:** XRF core scanner analyses. **Evelyne Talès:** Review & Editing.

Acknowledgements

Funding: This work was supported by the University of Paris-Est Creteil and the Piren-Seine axis 3 of phase 8 of the PIREN-Seine (https://www.piren-seine.fr/) in the framework of the sub-axis 'Trajectory of peri-urban rivers'. The authors of this article would like to thank the *Parc Naturel Régional de la Haute vallée de Chevreuse* and the Yvelines departmental council for their collaboration in this study and particularly the access to the field. We are also grateful to Axel Beauchamp, Thomas Depret, Claude Legentil and Annaëlle Vayssière for help in the field.

Data Availability Statement

All data are available from the corresponding author upon request.

References

Antoine, P., Fagnart, J.P., Limondin-Lozouet, N., Munaut, A.V., 2000. Le Tardiglaciaire du bassin de la Somme : éléments de synthèse et nouvelles données. Quaternaire 11(2), 85–98. https://doi.org/10.3406/quate.2000.1658

Arnaud, F., Révillon, S., Debret, M., Revel, M., Chapron, E., Jacob, J., Giguet-Covex, C., Poulenard, J., Magny, M., 2012. Lake Bourget regional erosion patterns reconstruction reveals Holocene NW European Alps soil evolution and paleohydrology. Quaternary Science Reviews 51, 81–92. https://doi.org/10.1016/j.quascirev.2012.07.025

Bakker M., van Smeerdijk D.G., 1982. A palaeoecological study of a Late Holocene section from « Het Ilperveld », western Netherlands. Review of Palaeobotany and Palynology 36 (1-2), 95-163. https://doi.org/10.1016/0034-6667(82)90015-X

Barthelmes A., Prager A., Joosten H., 2006. Palaeoecological analysis of Alnus wood peats with special attention to non-pollen palynomorphs. Review of Palaeobotany and Palynology 141 (1-2), 33-51. https://doi.org/10.1016/j.revpalbo.2006.04.002

Beauchamp, A., Lespez, L., Delahaye, D., 2017a. Impacts des aménagements hydrauliques sur les systèmes fluviaux bas-normands depuis 2000 ans, premiers résultats d'une approche

géomorphologique et géoarchéologique dans la moyenne vallée de la Seulles. Quaternaire 28(2), 253–258. https://doi.org/10.4000/quaternaire.8153
Beauchamp, A., Lespez, L., Rollet, A.-J., Germain-Vallée, C., Delahaye, D., 2017b. Les transformations anthropiques d'un cours d'eau de faible énergie et leurs conséquences, approche géomorphologique et géoarchéologique dans la moyenne vallée de la Seulles, Normandie. Géomorphologie : relief, processus, environnement 23(2), 121-138. https://doi.org/10.4000/geomorphologie.11702
Behre K.E., 1981. The interpretation of anthropogenic indicators in pollen diagrams. Pollen et Spores 23 (2), 225-245.
Behre K.-E., 1988. The rôle of man in European vegetation history. In Huntley B, Webb T. III (Eds), Vegetation History, Kluwer Academic Publishers 7, 633-672. https://doi.org/10.1007/978-94-009-3081-0_17
Benoit, P., 2000. L'alimentation et les usages de l'eau à Paris du XIIe au XVIe siècle. Rapport d'activité du PIREN-Seine 28, 1-8.
Benoit, P., Berthier, K., Billen, G., Lechevallier, G., 2003. Eau, industries et pollution dans le bassin de la Seine. Rapport d'activité du PIREN-Seine 33, 1-13.
Bensaadoune, S., Gentili, F., Pastre, J.-F., Gauthier, A., 2005. Les aménagements hydrauliques du bassin amont du Crould (Val d'Oise) : perceptions stratigraphiques de leurs impacts environnementaux. Estuaria 7, 67–82.
Berglund B., Persson T., Emanuelsson U., Persson S., 1986. Pollen/vegetation relationships in grazed and mowed plant communities of South Sweden. In Behre K.E. (Ed), Anthropogenic indicators in pollen diagrams. A.A. Balkema, Rotterdam, Boston, 37-51.
Berthier, K., 2007. Usages, gestion et industrialisation de la Bièvre dans le Val-de-Marne de l'antiquité à nos jours. 18ème Journées Scientifiques de l'Environnement. Environnement, Citoyenneté et Territoires Urbains, 1-19.
Beug H.J., 2004. Leitfaden der Pollenbestimmung für Mitteleuropa und angrenzende Gebiete. Verlag Dr. Friedrich Pfeil, München, 542.
Birks H.J.B., Birks H.H., 1980. Quaternary palaeoecology. Edward Arnold, London.
Blaauw, M., Christen, J., 2011. Flexible paleoclimate age-depth models using an autoregressive gamma process. Bayesian Analysis 6. https://doi.org/10.1214/ba/1339616472
Blancquaert, G., Leroyer, C., Lorho, T., Malrain F., Zech-Matterne, V., 2012. Rythmes de créations et d'abandons des établissements ruraux du second âge du Fer et interactions environnementales. pp. 213–220.
Blott, S.J., Pye, K., 2001. GRADISTAT: a grain size distribution and statistics package for the analysis of unconsolidated sediments. Earth Surface Processes and Landforms 26 (11), 1237–1248. https://doi.org/10.1002/esp.261
Bourlet, C., Layec, A., 2013. Densités de population et socio-topographie : la géolocalisation du rôle de taille de 1300. In : Paris, de Parcelles en pixels, Analyse géomatique de l'espace parisien médiéval et moderne, 223–246.
Bournerias M., Arnal G., Bock C., 2001. Guide des groupements végétaux de la région parisienne, 4ème ed. Belin, Paris.
Bradshaw E.G., Rasmussen P., Nielsen H., Anderson N.J., 2005. Mid- to late-Holocene land-use change and lake development at Dallund Sø, Denmark: trends in lake primary production as reflected by algal and macrophyte remains. The Holocene 15(8), 1130-1142. https://doi.org/10.1191/0959683605hl887rp
Bradshaw R.H.W., Coxon P., Greig J.R.A., Hall A.R., 1981. New fossil evidence for the past cultivation and processing of hemp (Cannabis sativa L.) in eastern England. New Phytologist 89(3), 503-510. https://doi.org/10.1111/j.1469-8137.1981.tb02331.x
Bronk Ramsey, C.B., 2017. Methods for Summarizing Radiocarbon Datasets. Radiocarbon 59(6), 1809–1833. https://doi.org/10.1017/RDC.2017.108
Broothaerts, N., Swinnen, W., Hoevers, R., Verstraeten, G., 2021. Changes in floodplain geo-ecology in the Belgian loess belt during the first millennium AD. Netherlands Journal of Geosciences 100 (e14), 1-12. https://doi.org/10.1017/njg.2021.9
Broothaerts, N., Verstraeten, G., Kasse, C., Bohncke, S., Notebaert, B., Vandenberghe, J., 2014. Reconstruction and semi-quantification of human impact in the Dijle catchment, central Belgium: a

palynological and statistical approach. Quaternary Science Reviews 102, 96–110. https://doi.org/10.1016/j.quascirev.2014.08.006
Brown, A.G., 2009. Colluvial and alluvial response to land use change in Midland England: An integrated geoarchaeological approach. Geomorphology 108, 92–106. https://doi.org/10.1016/j.geomorph.2007.12.021
Brown, A.G., 1997. Alluvial Geoarchaeology: Floodplain Archaeology and Environmental Change, Cambridge Manuals in Archaeology. Cambridge University Press, Cambridge. https://doi.org/10.1017/CBO9780511607820
Brown, A.G., Lespez, L., Sear, D.A., Macaire, J.-J., Houben, P., Klimek, K., Brazier, R.E., Van Oost, K., Pears, B., 2018. Natural vs anthropogenic streams in Europe: History, ecology and implications for restoration, river-rewilding and riverine ecosystem services. Earth-Science Reviews 180, 185–205. https://doi.org/10.1016/j.earscirev.2018.02.001
Carrión J.S., 2002. Patterns and processes of Late Quaternary environmental change in a montane region of southwestern Europe. Quaternary Science Reviews 21, 2047-2066.
Chaussé, C., Leroyer, C., Girardclos, O., Allenet, G., Pion, P., Raymond, P., 2008. Holocene history of the River Seine, Paris, France: bio-chronostratigraphic and geomorphological evidence from the Quai-Branly. The Holocene 18, 967–980. https://doi.org/10.1177/0959683608093535
Chin, A., 2006. Urban transformation of river landscapes in a global context. Geomorphology 79, 460–487. https://doi.org/10.1016/j.geomorph.2006.06.033
Cour P., 1974. Nouvelles techniques de détection des flux et des retombées polliniques : étude de la sédimentation des pollens et des spores à la surface du sol. Pollen et Spores 16 (1), 103–141.
Csiki, S., Rhoads, B.L., 2010. Hydraulic and geomorphological effects of run-of-river dams. Progress in Physical Geography: Earth and Environment 34, 755–780. https://doi.org/10.1177/0309133310369435
Cugny C., 2011. Apports des microfossiles non-polliniques à l'histoire du pastoralisme sur le versant nord pyrénéen. Entre référentiels actuels et reconstitution du passé. Thèse de doctorat, Université Toulouse 2.
David, R., Leroyer, C., Mazier, F., Lanos, P., Dufresne, P., 2012. Les transformations de la végétation du bassin parisien par la modélisation des données polliniques holocènes, 53-68. https://hal.archives-ouvertes.fr/hal-01171988
Davison, W., 1993. Iron and manganese in lakes. Earth-Science Reviews 34, 119–163. https://doi.org/10.1016/0012-8252(93)90029-7
de Moor, J.J.W., Kasse, C., van Balen, R., Vandenberghe, J., Wallinga, J., 2008. Human and climate impact on catchment development during the Holocene — Geul River, the Netherlands. Geomorphology, Human and climatic impacts on fluvial and hillslope morphology 98, 316–339. https://doi.org/10.1016/j.geomorph.2006.12.033
Dearing, J.A., Hay, K.L., Baban, S.M.J., Huddleston, A.S., Wellington, E.M.H., Loveland, P.J., 1996. Magnetic susceptibility of soil: an evaluation of conflicting theories using a national data set. Geophysical Journal International 127, 728–734. https://doi.org/10.1111/j.1365-246X.1996.tb04051.x
Dmitrieva, T., Lestel, L., Meybeck, M., Barles, S., 2018. Versailles facing the degradation of its water supply from the Seine River: governance, water quality expertise and decision making, 1852–1894. Water Hist 10, 183–205. https://doi.org/10.1007/s12685-018-0216-7
Donovan, M., Miller, A., Baker, M., 2016. Reassessing the role of milldams in Piedmont floodplain development and remobilization. Geomorphology 268, 133–145. https://doi.org/10.1016/j.geomorph.2016.06.007
Donovan, M., Miller, A., Baker, M., Gellis, A., 2015. Sediment contributions from floodplains and legacy sediments to Piedmont streams of Baltimore County, Maryland. Geomorphology 235, 88–105. https://doi.org/10.1016/j.geomorph.2015.01.025
Dow, S., Snyder, N.P., Ouimet, W.B., Martini, A.M., Yellen, B., Woodruff, J.D., Newton, R.M., Merritts, D.J., Walter, R.C., 2020. Estimating the timescale of fluvial response to anthropogenic disturbance using two generations of dams on the South River, Massachusetts, USA. Earth Surf. Process. Landforms 45, 2380–2393. https://doi.org/10.1002/esp.4886
Downward, S., Skinner, K., 2005. Working rivers: the geomorphological legacy of English freshwater mills. Area 37, 138–147. https://doi.org/10.1111/j.1475-4762.2005.00616.x
Enevold R., Rasmussen P., Løvschal M., Olsen J., Odgaard B.V., 2019. Circumstantial evidence of non-pollen palynomorph palaeoecology: a 5,500-year NPP record from forest hollow sediments compared

to pollen and macrofossil inferred palaeoenvironments. Vegetation History and Archaeobotany 28, 105-121. https://doi.org/10.1007/s00334-018-0687-6
Fernez T., Lafon P., Hendoux F., 2015. Guide des végétations remarquables de la région Île-de-France. Conservatoire botanique national du Bassin parisien, DRIEE d'Île-de-France, Paris.
Frioux, S., 2010b. Fléau, ressource, exutoire : visions et usages des rivières urbaines (XVIIIe-XXIe s.). Géocarrefour 188–192.
Gaillard M.-J., Dearing J.A., El-Daoushy F., Enell M., Håkansson H., 199-1. A late Holocene record of land-use history, soil erosion, lake trophy and lake-level fluctuations at Bjäresjösjön (South Sweden). Journal of Paleolimnology 6, 51-81.
Gelorini V., 2011. Diversity and palaeoecological significance of non-pollen palynomorph assemblages in East African lake sediments. Thesis, Faculty of Sciences, Universiteit Gent.
Gordon A.D., Birks H.J.B., 1972. Numerical methods in Quaternary palaeoecology. I. Zonation of pollen diagrams. New Phytologist 71, 961-979.
Granai, S., Limondin-Lozouet, N., 2014. Contribution of two malacological successions from the Seine floodplain (France) in the reconstruction of the Holocene palaeoenvironmental history of northwest and central Europe: vegetation cover and human impact. Journal of Archaeological Science 52, 468–482. https://doi.org/10.1016/j.jas.2014.09.011
Grönlund E., Simola H., Huttunen P., 1986. Paleolimnological reflections of fiber-plant retting in the sediment of a small clear water lake. Hydrobiologia 143, 425-431.
Guillerme, A., 1983. Les temps de l'eau : la cité, l'eau et les techniques : nord de la France : fin IIIe-début XIXe siècle. Editions Champ Vallon.
Guiry M.D., Guiry G.M., 2022. AlgaeBase. World-wide electronic publication, National University of Ireland, Galway. http://www.algaebase.org; searched on 11 June 2021 and 24 March 2022.
Hall V.A., 1994. Landscape development in northeast Ireland over the last half millenium. Review of Palaeobotany and Palynology 82, 75-82.
Hillbrand M., Hadorn P., Cugny C., Hasenfratz A., Galop D., Haas J.N., 2012. The palaeoecological value of Diporotheca rhizophila ascospores (Diporotheaceae, Ascomycota) found in Holocene sediments from Lake Nussbaumersee, Switzerland. Review of Palaeobotany and Palynology 186, 62-68.
Houben, P., Schmidt, M., Mauz, B., Stobbe, A., Lang, A., 2013. Asynchronous Holocene colluvial and alluvial aggradation: A matter of hydrosedimentary connectivity. The Holocene 23, 544–555. https://doi.org/10.1177/0959683612463105
Huntley B., Birks H.J.B., 1983. An atlas of past and present pollen maps for Europe: 0-13000 years ago. Cambridge University Press, Cambridge.
Inamdar, S., Peipoch, M., Gold, A.J., Lewis, E., Hripto, J., Sherman, M., Addy, K., Merritts, D., Kan, J., Groffman, P.M., Walter, R., Trammell, T.L.E., 2021. Ghosts of landuse past: legacy effects of milldams for riparian nitrogen (N) processing and water quality functions. Environ. Res. Lett. 16, 035016. https://doi.org/10.1088/1748-9326/abd9f5
Innes J.B., Blackford J.J., 2003. The ecology of late Mesolithic woodland disturbances: model testing with fungal spore assemblage data. Journal of Archaeological Science 30, 185-194.
John D.M., Whitton B.A., Brook A.J. (Eds), 2002. The freshwater algal flora of the British Isles: an identification guide to freshwater and terrestrial algae. Cambridge University Press.
Jugie M. 2018. Trajectoire hydrogéomorphologique d'un petit cours d'eau périurbain francilien. Aménagement, « désaménagement » ?, Theisis, Université Paris I Sorbone Panthéon, , 466. ⟨tel-02181434⟩.
Jugie, M., Gob, F., Le Coeur, C., 2017. Restauration de la continuité écologique. Trajectoire hydrosédimentaire d'une rivière aménagée, la Mérantaise. Rapport d'activité du PIREN-Seine, 1-28.
Jugie, M., Gob, F., Virmoux, C., Brunstein, D., Tamisier, V., Le Coeur, C., Grancher, D., 2018. Characterizing and quantifying the discontinuous bank erosion of a small low energy river using Structure-from-Motion Photogrammetry and erosion pins. Journal of Hydrology 563, 418–434. https://doi.org/10.1016/j.jhydrol.2018.06.019
Kalicki, T., Przepióra, P., Kusztal, P., Chrabąszcz, M., Fularczyk, K., Kłusakiewicz, E., Frączek, M., 2020. Historical and present-day human impact on fluvial systems in the Old-Polish Industrial District (Poland). Geomorphology 357, 107062. https://doi.org/10.1016/j.geomorph.2020.107062

Kuhry P., 1997. The palaeoecology of a treed bog in western boreal Canada: a study based on microfossils, macrofossils and physico-chemical properties. Review of Palaeobotany and Palynology 96, 183-224.
Kylander, M.E., Ampel, L., Wohlfarth, B., Veres, D., 2011. High-resolution X-ray fluorescence core scanning analysis of Les Echets (France) sedimentary sequence: new insights from chemical proxies: XRF core scanning analysis of les echets sedimentary sequence. Journal of Quaternary Science 26, 109–117. https://doi.org/10.1002/jqs.1438
Lagerås P., 1996. Long-term history of land-use and vegetation at Femtingagölen – a small lake in the Småland Uplands, southern Sweden. Vegetation History and Archaeobotany 5, 215-228.
Lagerås P., Jansson K., Vestbö A, 1995. Land-use history of the Axlarp area in the Småland uplands, southern Sweden: palaeoecological and archaeological investigations. Vegetation History and Archaeobotany 4, 223-234.
Laine A., Gauthier E., Garcia J.-P., Petit C., Cruz F., Richard H., 2010. A three-thousand-year history of vegetation and human impact in Burgundy (France) reconstructed from pollen and non-pollen palynomorphs analysis. Comptes Rendus Biologies 333, 850-857.
Larsson M., Lagerås P., 2015. New evidence on the introduction, cultivation and processing of hemp (Cannabis sativa L.) in southern Sweden. Environmental Archaeology 20 (2), 111-119.
Larue, J.-P., Etienne, R., 2000. Les Sables de Lozère dans le Bassin parisien : nouvelles interprétations 2(6), 81-94.
Latałowa M., 1992. Man and vegetation in the pollen diagrams from Wolin Island (NW Poland). Acta Palaeobotanica 32 (1), 123-249.
Lavrieux M., Jacob J., Disnar J.-R., Bréheret J.-G., Le Milbeau C., Miras Y., Andrieu-Ponel V., 2013. Sedimentary cannabinol tracks the history of hemp retting. Geology 41 (7), 751-754.
Le Jeune, Y., Leroyer, C., Pastre, J.-F., 2012. L'évolution holocène de la basse vallée de la Marne (Bassin parisien, France) entre influences climatiques et anthropiques. Géomorphologie : relief, processus, environnement 4, 459–476. https://doi.org/10.4000/geomorphologie.10060
Le Roux, T., 2010. Une rivière industrielle avant l'industrialisation : la Bièvre et le fardeau de la prédestination, 1670-1830. Géocarrefour 193–207. https://doi.org/10.4000/geocarrefour.7952
Leroyer C., 1997. Homme, Climat, Végétation au Tardi-et-Postglaciaire dans le Bassin parisien : apports de l'étude palynologique des fonds de vallée, thèse de doctorat, Université de Paris I- Panthéon - Sorbonne, 786 p.
Leroyer, C., Allenet, G., 2006. L'anthropisation du paysage végétal d'après les données polliniques : l'exemple des fonds de vallées du Bassin parisien, in: L'Érosion entre Société, Climat et Paléoenvironnement. Actes de la table ronde en l'honneur de R. Neboit Guilhot, 65-74.
Lespez, L., Clet-Pellerin, M., Limondin-Lozouet, N., Pastre, J.-F., Fontugne, M., Marcigny, C., 2008. Fluvial system evolution and environmental changes during the Holocene in the Mue valley (Western France). Geomorphology 98, 55–70. https://doi.org/10.1016/j.geomorph.2007.02.029
Lespez, L., Germaine, M.-A., 2016. La rivière désaménagée ? Les paysages fluviaux et l'effacement des seuils et des barrages en europe de l'ouest et en amérique du nord-est. Bulletin de la Société Géographique de Liège 67, 223-254. https://doi.org/10.25518/0770-7576.4465
Lespez, L., Viel, V., Rollet, A.J., Delahaye, D., 2015. The anthropogenic nature of present-day low energy rivers in western France and implications for current restoration projects. Geomorphology 251, 64–76. https://doi.org/10.1016/j.geomorph.2015.05.015
Lewin, J., 2010. Medieval environmental impacts and feedbacks: The lowland floodplains of England and Wales. Geoarchaeology 25, 267–311. https://doi.org/10.1002/gea.20308
Loke, M.H., Barker, R.D., 1996. Rapid least-squares inversion of apparent resistivity pseudosections by a quasi-Newton method1. Geophysical Prospecting 44, 131–152. https://doi.org/10.1111/j.1365-2478.1996.tb00142.x
Lu, Y., Fritz, S.C., Stone, J.R., Krause, T.R., Whitlock, C., Brown, E.T., Benes, J.V., 2017. Trends in catchment processes and lake evolution during the late-glacial and early- to mid-Holocene inferred from high-resolution XRF data in the Yellowstone region. J Paleolimnol 58, 551–569. https://doi.org/10.1007/s10933-017-9991-x
Mauch, C., Zeller, T., 2008. Rivers in History: Perspectives on Waterways in Europe and North America. University of Pittsburgh Press.

Mercuri A.M., Accorsi C.A., Mazzanti M.B., 2002. The long history of Cannabis and its cultivation by the Romans in central Italy, shown by pollen records from Lago Albano and Lago di Nemi. Vegetation History and Archaeobotany 11, 263-276.
Miras Y., Beauger A., Lavrieux M., Berthon V., Serieyssol K., Andrieu-Ponel V., Ledger P.M., 2015. Tracking long-term human impacts on landscape, vegetal biodiversity and water quality in the Lake Aydat catchment (Auvergne, France) using pollen, non-pollen palynomorphs and diatom assemblages. Palaeogeography, Palaeoclimatology, Palaeoecology 424, 76-90.
Moore P.D., Webb J.A., Collinson M.E., 1991. Pollen analysis, 2nd ed. Blackwell Scientific Publications, Oxford.
Maaß, A.-L., Schüttrumpf, H., 2019. Elevated floodplains and net channel incision as a result of the construction and removal of water mills. Geografiska Annaler: Series A, Physical Geography 101, 157–176. https://doi.org/10.1080/04353676.2019.1574209
Maaß, A.-L., Schüttrumpf, H., Lehmkuhl, F., 2019. Looking back, looking forward: Human impacts on fluvial morphodynamics since the Industrial Revolution and the return to a natural morphological river state (No. RWTH-2019-08256). Dissertation, Rheinisch-Westfälische Technische Hochschule Aachen, 2019.
Marchandin, P., 2021. Moulins et énergie à Paris du XIIIe au XVIe siècle. Thesis, Université Paris sciences et lettres. theses.hal.science/tel-03174895
Mazian, B., 2018. Approche intégrée du procédé de rouissage des fibres de chanvre : Vers une amélioration de la qualité des intrants pour la fabrication des matériaux biocomposites. Mines Alès Ecole des Mines.
Merritts, D., Walter, R., Rahnis, M., Cox, S., Hartranft, J., Scheid, C., Potter, N., Jenschke, M., Reed, A., Matuszewski, D., Kratz, L., Manion, L., Shilling, A., Datin, K., 2013. The rise and fall of Mid-Atlantic streamsMillpond sedimentation, milldam breaching, channel incision, and stream bank erosion, in: The Challenges of Dam Removal and River Restoration. Geological Society of America. https://doi.org/10.1130/2013.4121(14)
Merritts, D., Walter, R., Rahnis, M., Hartranft, J., Cox, S., Gellis, A., Potter, N., Hilgartner, W., Langland, M., Manion, L., Lippincott, C., Siddiqui, S., Rehman, Z., Scheid, C., Kratz, L., Shilling, A., Jenschke, M., Datin, K., Cranmer, E., Becker, S., 2011. Anthropocene Streams and Base-Level Controls from Historic Dams in the Unglaciated Mid-Atlantic Region, USA. Philosophical transactions. Series A, Mathematical, physical, and engineering sciences 369, 976–1009. https://doi.org/10.1098/rsta.2010.0335
Milsom, 2011. Field Geophysics, 4th Edition, 4th Edition. ed. Wiley, Hoboken, NJ.
Notebaert, B., Broothaerts, N., Verstraeten, G., 2018. Evidence of anthropogenic tipping points in fluvial dynamics in Europe. Global and Planetary Change 164, 27–38. https://doi.org/10.1016/j.gloplacha.2018.02.008
Notebaert, B., Verstraeten, G., 2010. Sensitivity of West and Central European River systems to environmental changes during the Holocene: A review. Earth-Science Reviews 103, 163–182. https://doi.org/10.1016/j.earscirev.2010.09.009
Orth, P., Pastre, J.F., Gauthier, A., Limondin-Lozouet, N., Kunesch, S., 2004. Les enregistrements morphosédimentaires et biostratigraphiques des fonds de vallée du bassin-versant de la Beuvronne (Bassin parisien, Seine-et-Marne, France) : perception des changements climatoanthropiques à l'Holocène. Quaternaire 15, 285–298. https://doi.org/10.3406/quate.2004.1775
Pals J.P., van Geel B., Delfos A., 1980. Paleoecological studies in the Klokkeweel bog near Hoogkarspel (prov. Of Noord-Holland). Review of Palaeobotany and Palynology 30, 371-418.
Peglar S.M., Fritz S.C., Birks H.J.B., 1989. Vegetation and land-use history at Diss, Norfolk, U.K. Journal of Ecology 77, 203-222.
Prager A., Theuerkauf M., Couwenberg J., Barthelmes A., Aptroot A., Joosten H., 2012. Pollen and non-pollen palynomorphs as tools for identifying alder carr deposits: a surface sample study from NE-Germany. Review of Palaeobotany and Palynology 186, 38-57.
Pastre, J.-F., 2018. L'évolution tardiglaciaire et holocène du bassin du Crould (Val d'Oise). Revue archéologique d'Île-de-France, RAIF - Supplément 5 - 2018 21–36.
Pastre, J.F., Leroyer, C., Limondin-Lozouet, N., Orth, P., Chaussé, C., Fontugne, M., Gauthier, A., Kunesch, S., Le Jeune, Y., Saad, M.-C., 2002. Variation paléoenvironnementale et paléohydrologiques durant les 15 derniers millénaires : les réponses morphosédimentaires des vallées du Bassin Parisien

(France), in : Les fleuves ont une histoire : paléoenvironnement des rivières et des lacs français depuis 15000 ans, Archéologie aujourd'hui. Editions Errance, 29-44.
Pastre, J.-F., Orth, P., Le Jeune, Y., Bensaadoune, S., 2006. L'homme et l'érosion dans le Bassin parisien (France). La réponse des fonds de vallée au cours de la seconde partie de l'Holocène, in : L'Érosion entre Société, Climat et Paléoenvironnement, actes de la table ronde en l'honneur de R. Neboit Guilhot, 237–247.
Poeppl, R.E., Keesstra, S.D., Hein, T., 2015. The geomorphic legacy of small dams—An Austrian study. Anthropocene 10, 43–55. https://doi.org/10.1016/j.ancene.2015.09.003
Rasmussen P., 2005. Mid-to late-Holocene land-use change and lake development at Dallund Sø, Denmark: vegetation and land-use history inferred from pollen data. The Holocene 15 (8), 1116-1129.
Reille M., 1992. Pollen et spores d'Europe et d'Afrique du Nord. Laboratoire de Botanique historique et Palynologie, Marseille.
Reille M., 1995. Pollen et spores d'Europe et d'Afrique du Nord, Supplément 1. Laboratoire de Botanique historique et Palynologie, Marseille.
Reille M., 1998. Pollen et spores d'Europe et d'Afrique du Nord, Supplément 2. Laboratoire de Botanique historique et Palynologie, Marseille.
Reinbold A., 2017. Dynamiques de la végétation et structuration des paysages. Etude interdisciplinaire des paysages agropastoraux des campagnes médiévales du nord de la Haute-Bretagne (XIe-XVIe s.). Thèse de doctorat, Université Rennes 2.
Revelles J., Burjachs F., van Geel B., 2016. Pollen and non-pollen palynomorphs from the Early Neolithic settlement of La Draga (Girona, Spain). Review of Palaeobotany and Palynology 225, 1-20.
Revelles J., van Geel B., 2016. Human impact and ecological changes in lakeshore environments. The contribution of non-pollen palynomorphs in Lake Banyoles (NE Iberia). Review of Palaeobotany and Palynology 232, 81-97.
Riera S., López-Sáez J.A., Julià R., 2006. Lake responses to historical land use changes in northern Spain: The contribution of non-pollen palynomorphs in a multiproxy study. Review of Palaeobotany and Palynology 141, 127-137.
Reimer, P.J., Austin, W.E.N., Bard, E., Bayliss, A., Blackwell, P.G., Ramsey, C.B., Butzin, M., Cheng, H., Edwards, R.L., Friedrich, M., Grootes, P.M., Guilderson, T.P., Hajdas, I., Heaton, T.J., Hogg, A.G., Hughen, K.A., Kromer, B., Manning, S.W., Muscheler, R., Palmer, J.G., Pearson, C., Plicht, J. van der, Reimer, R.W., Richards, D.A., Scott, E.M., Southon, J.R., Turney, C.S.M., Wacker, L., Adolphi, F., Büntgen, U., Capano, M., Fahrni, S.M., Fogtmann-Schulz, A., Friedrich, R., Köhler, P., Kudsk, S., Miyake, F., Olsen, J., Reinig, F., Sakamoto, M., Sookdeo, A., Talamo, S., 2020. The IntCal20 Northern Hemisphere Radiocarbon Age Calibration Curve (0–55 cal kBP). Radiocarbon 62, 725–757. https://doi.org/10.1017/RDC.2020.41
Reynolds, J.M., 2011. An Introduction to Applied and Environmental Geophysics, 2nd Edition. ed. Wiley–Blackwell, Chichester, West Sussex; Malden, Mass.
Rouillard, J., Benoit, P., Morera, R. 2011. L'eau dans les campagnes du bassin de la Seine avant l'ère industrielle, Fascicule PIREN, 10, Paris.
Sapin M.-L., Virassamy C., 2020. Les savoir-faire du chanvre textile. L'inventaire national du Patrimoine culturel immatériel, 2020_67717_INV_PCI_FRANCE_00481, https://www.culture.gouv.fr/Thematiques/Patrimoine-culturel-immateriel/Le-Patrimoine-culturel-immateriel/L-inventaire-national-du-Patrimoine-culturel-immateriel.
Schofield J.E., Waller M.P., 2005. A pollen analytical record for hemp retting from Dungeness Foreland, UK. Journal of Archaeological Science 32, 715-726.
Shumilovskikh L.S., Shumilovskikh E.S., Schlütz F., van Geel B., 2021. NPP-ID: Non-Pollen Palynomorph Image Database as a research and educational platform. Vegetation History and Archaeobotany. https://doi.org/10.1007/s00334-021-00849-8.
Sieber T.N., Sieber-Canavesi F., Dorworth C.E., 1991. Endophytic fungi of red alder (Alnus rubra) leaves and twigs in British Columbia. Canadian Journal of Botany 69, 407-411.
Schenk, E.R., Hupp, C.R., 2009. Legacy Effects of Colonial Millponds on Floodplain Sedimentation, Bank Erosion, and Channel Morphology, Mid-Atlantic, USA1. JAWRA Journal of the American Water Resources Association 45, 597–606. https://doi.org/10.1111/j.1752-1688.2009.00308.x
Schroeder, M., 2019. The history of European hemp cultivation. Dissertations in Geology at Lund University.

1476 Skalak, K., Pizzuto, J., Hart, D.D., 2009. Influence of Small Dams on Downstream Channel
1477 Characteristics in Pennsylvania and Maryland: Implications for the Long-Term Geomorphic Effects of
1478 Dam Removal1. JAWRA Journal of the American Water Resources Association 45, 97–109.
1479 https://doi.org/10.1111/j.1752-1688.2008.00263.x
1480 Stephan E. 2007. Le Domaine d'Ors à Châteaufort. Bulletin de la société historique et archéologique de
1481 Rambouillet et de l'Yvelines, SHARY, 104, 17-31.
1482 Tulippe, O., 1934. L'habitat rural en Seine-et-Oise. Essai de géographie du peuplement. Université de
1483 Liège.
1484 van Geel B., 1978. A palaeoecological study of Holocene peat bog sections in Germany and The
1485 Netherlands. Review of Palaeobotany and Palynology 25, 1-120.
1486 van Geel B., 1986. Application of fungal and algal remains and other microfossils in palynological
1487 analyses. In: Berglund B.E. (Ed.), Handbook of Holocene palaeoecology and Palaeohydrology. John
1488 Wiley & Sons, pp. 497-505.
1489 van Geel B., 2001. Non pollen palynomorphs. In Smol J.P., Birks H.J.B., W.M. Last (Eds.), Tracking
1490 Environmental Change Using Lake Sediments, vol. 3. Kluwer Academic Publishers, Dordrecht, pp.
1491 99-119.
1492 van Geel B., Hallewas D.P., Pals J.P., 1982/1983. A Late Holocene deposit under the Westfriese Zeedijk
1493 near Enkhuizen (Prov. Of Noord-Holland, The Netherlands): palaeoecological and archaeological
1494 aspects. Review of Palaeobotany and Palynology 38, 269-335.
1495 van Geel B., Coope G.R., van der Hammen T., 1989. Palaeoecology and stratigraphy of the Lateglacial
1496 type section at Usselo (The Netherlands). Review of Palaeobotany and Palynology 60, 25-129.
1497 van Geel B., Mur L.R., Ralska-Jasiewiczowa M., Goslar T., 1994. Fossil akinetes of Aphanizomenon and
1498 Anabaena as indicators for medieval phosphate-eutropication of Lake Gosciaz (Central Poland).
1499 Review of Palaeobotany and Palynology 83, 97-105.
1500 van Geel, B., Odgaard, B.V. and Ralska-Jasiewiczowa, M., 1996. Cyanobacteria as indicators of
1501 phosphate-eutrophication of lakes and pools in the past. Pact 50 (IV.5), 399–415.
1502 van Geel B., Aptroot A., 2006. Fossil Ascomycetes in Quaternary deposits. Nova Hedwigia 82 (3-4), 313-
1503 329.
1504 van Smeerdijk D.G., 1989. A palaeoecological and chemical study of a peat profile from the Assendelver
1505 Polder (The Netherlands). Review of Palaeobotany and Palynology 58, 231-288.
1506 Vuorela I., 1973. Relative pollen rain around cultivated fields. Acta Botanica Fennica 102, 1-27.
1507 Verosub, K.L., Roberts, A.P., 1995. Environmental magnetism: Past, present, and future. J. Geophys.
1508 Res. 100, 2175–2192. https://doi.org/10.1029/94JB02713
1509 Verstraeten, G., Broothaerts, N., Van Loo, M., Notebaert, B., D'Haen, K., Dusar, B., De Brue, H., 2017.
1510 Variability in fluvial geomorphic response to anthropogenic disturbance. Geomorphology,
1511 Anthropogenic Sedimentation 294, 20–39. https://doi.org/10.1016/j.geomorph.2017.03.027
1512 Walsh, C.J., Fletcher, T.D., Bos, D.G., Imberger, S.J., 2015. Restoring a stream through retention of
1513 urban stormwater runoff: a catchment-scale experiment in a social–ecological system. Freshwater
1514 Science 34, 1161–1168. https://doi.org/10.1086/682422
1515 Walter, R.C., Merritts, D.J., 2008. Natural Streams and the Legacy of Water-Powered Mills. Science 319,
1516 299–304. https://doi.org/10.1126/science.1151716
1517 Whittington G., Edwards K.J., 1989. Problems in the interpretation of Cannabaceae pollen in the
1518 stratigraphic record. Pollen et Spores 31 (1-2), 79-96.
1519 Xu Zhou, K., Ionescu, A., Wan, E., Ho, Y.N., Barnes, C.H.W., Christie, G., Wilson, D.I., 2018.
1520 Paramagnetism in Bacillus spores: Opportunities for novel biotechnological applications. Biotechnol.
1521 Bioeng. 115, 955–964. https://doi.org/10.1002/bit.26501